THE INVESTIGATION OF INDUCTION MOTOR CHARACTERISTICS BY MEANS OF A MICROWAVE TECHNIQUE

BY

U.M. KAPLAN

Thesis submitted to the
Department of Electrical Engineering
of the University of Cape Town
for the degree of
Doctor of Philosophy

1963

SUMMARY.

An apparatus capable of following the rapid variations in torque and speed produced by an induction motor under starting conditions was designed and constructed. Its performance and results obtained are given.

The deviation of the actual torque characteristics of an induction motor from the theoretical characteristic is investigated, with the treatment separated into two sections. The first section deals with the torque produced during the acceleration over the range slip = 2 to slip = zero, excluding any switching transients, and verifies the possibility of transient overspeeding in the case of rapid acceleration. The discontinuity of the torque characteristic over the stand-still region is clearly shown and a further investigation to obtain conclusive results is outlined.

The second section of the investigation deals with the torque produced under switching transient conditions. The fact that torque pulsations are produced during the existence of the transient switching currents and fluxes is verified. These torque pulsations are shown to be produced by the actions and interactions of three sets of quantities which are,

a) The steady state stator quantities,

b) a set of stator adherent transient quantities and

c) a set of rotor adherent transient quantities.

Under conditions where the rotor adherent transient quantities decay rapidly relative to the stator adherent transient quantities, the frequency of the torque pulsations is mainly that of the supply, while under conditions where the stator adherent transient quantities decay rapidly relative to the rotor adherent transient quantities, as in the case of a squirrel cage induction motor, the frequency of the torque pulsations is shown to be equal to the frequency of slip of the rotor relative to the steady state stator revolving quantities.

The results are correlated with those obtained by previous investigators.

CONTENTS

1. INTRODUCTION.

The experimental investigation of the behaviour of induction motors during the starting period has to some extent been hampered by the lack of torque measuring apparatus capable of following the more rapid variations. For instance the influence of the transient currents of relatively short duration, which are initiated at the instant of connecting the stator to its source of supply, deserve further investigation.

The recording of the torque-speed characteristic of an induction motor, when using torque measuring apparatus with a relatively slow response, frequently requires the period of acceleration of the rotor to be increased by the addition of an inertia load. This practice fails in the case of an investigation into the influence of the above-mentioned transient currents. Firstly, these transient currents are of a finite duration which is relatively unaffected by an increase in the duration of the acceleration period, and secondly, as it will be shown, the frequency of torque variation under these conditions is governed primarily by the instantaneous velocity of the rotor relative to the synchronously revolving stator field.

Theoretical investigations of the behaviour of squirrel cage induction motors under transient conditions, based upon the equivalent two-phase theory of the induction machine developed by Stanley,[1] have been carried out by Gilfillan and Kaplan,[2] Weygandt and Charp[4] and Maggininis and Shultz.[5]

Weygandt and Charp confined their investigation to the current and speed of a two-phase induction motor during the accelerating period. Maggininis and Shultz have included the effect of mechanical transients produced by the sudden application of load to the motor in their investigation which concerns torque current and speed.

Gilfillan and Kaplan confined their investigation to the pulsations in torque produced by the action of transient currents initiated at switching, for the case where the rotor speed

was kept constant at slip = 2. The resulting calculated curves obtained, show that the magnitude of the pulsations in torque are from 200% to 400% of the steady accelerating torque and that the frequency of pulsation varies by up to ±25% of the supply frequency for a selection of motors in the commercial range.

These three sets of investigators used differential analyzers to provide solutions to the differential equations obtained.

Smith[3] and Rudenberg[18] have produced general theories based upon the summed quantities in a three-phase system to illustrate the production of transient currents fluxes and torques by the completion or interruption of the supply to a three-phase machine.

An experimental investigation of the torque pulsations produced by the transient currents initiated at the instant of switching has been carried out by Wahl and Kilgore.[6] This investigation was confined to the locked rotor case, and the measured results were checked theoretically. In this case the torque pulsations were of the order of 200% of the steady accelerating torque and the frequency of the pulsation was equal to that of the supply.

With the object of experimentally investigating the torque pulsations due to the transient switching currents over the speed range for which the rotor slip = 2 to zero, an apparatus has been designed and constructed with a frequency response in excess of 300 c.p.s., and provision has been made for the control of the speed and acceleration of the test motor over the above speed range.

As the torque measuring apparatus measures the reaction of the rotor torque on the stator, it is independent of the type of load or of the rotation of the rotor and is therefore suitable for investigating the complete torque/speed or torque/time characteristic of the induction motor.

The torque/time characteristics obtained, as will be shown later, are in general agreement with the familiar text-book forms of these characteristics. The results obtained from the investigation of the period of influence of the transient currents

initiated at switching substantiate the results obtained by Dahl and Kilgore for the locked rotor case, but differ from the calculated values of Gilfillan and Kaplan in so far as the frequency of torque pulsation at speeds other than stand-still is concerned.

The frequency of pulsation of these torques is shown to be dependent upon the velocity of the rotor relative to the synchronously revolving stator field during the period of influence of the transient switching currents. This phenomenon is investigated and explained in the latter half of the following treatise.

2. APPARATUS.

The final arrangement of the apparatus is shown in fig. 1 and a brief description of each portion and its function is given in table 1.

A more comprehensive description of the apparatus, dealing with the design and operation of each portion, where relevant, is presented in the immediately following sections.

TABLE 1. TABULATION OF APPARATUS.

UNIT	RELEVANT DATA	FUNCTION
Induction motor	1 h.p. 4 pole 1410 r.p.m. 3-phase 380 volt (star) 24 stator slots 33 rotor slots.	Test motor
D.C. motor	5 h.p. Ward-Leonard controlled, with dog-clutch connection to test motor.	Speed control
Tachometer	Homopolar generator with D.C. amplifier.	Speed measurement
Tuned cavity in a microwave system	Mechanically coupled to stator of test motor, fed from Klystron Oscillator, output to D.C. amplifier.	Torque measurement
Thyratron operated contactor	Firing pulse to thyratron grid supplied from a phase-shifting device.	Control of switching instant
Cathode ray oscilloscope		Recording device
Frequency trap	Series resonant circuit shunting c.r.o. input terminals.	Electrical damping of natural frequency vibrations

2.1. Design of motor suspension system.

It can be shown[7] that for a mechanical system having an inertia I (kgm-metres^2) about its axis of rotation and a specific restoring couple U (Newton-metres per radian) about that axis, the undamped natural frequency, f_o, of the system is

$$f_o = \frac{1}{2\pi}\sqrt{\frac{U}{I}} \text{ cycles per second} \quad \text{----------(1)}$$

For any applied force or torque with a period greater than $T_o = 1/f_o$ seconds it may be assumed that the system will attain its maximum deflection at the same instant at which the applied torque attains its maximum value. As the system will be stiffness controlled, provided T_o is less than the period of the applied torque, the magnitude of the deflections obtained will be proportional to the magnitude of the applied torque.

Where the period of the applied torque is less than T_o, the system will have a tendency to overshoot. This will result in the system only attaining a final steady deflection in a time dependent upon its inherent logarithmic damping coefficient. The logarithmic damping coefficient may be defined as the time taken for the vibrations, set up by an abruptly applied force or torque, to decay to 1/e of the initial amplitude of vibration. Alternatively, the logarithmic damping coefficient may be taken as being proportional to the inverse of the amplification factor, Q, of the system at its natural frequency, π being the coefficient of proportionality.

Furthermore as the system would be mass controlled when the period of the applied torque is less than T_o, the magnitude of any deflection would be dependent upon the period of the applied torque as well as its magnitude. In a mass controlled system the amplitude of deflection is proportional to the inverse of the square on the fractional increase in the frequency of vibration. For example, with the same magnitude of applied force, if the frequency of application is doubled, the amplitude of the vibration will be reduced to one-quarter of the previous value.

Consideration of the foregoing statements resulted in the decision to design the suspension system with as high a natural frequency as possible. The maximum value of the natural frequency is limited by the sensitivity of the deflection measuring device.

Initial estimates were made for the natural frequency and deflection limits, providing a means of assessing the suitability of the design of the suspension system. The values used were:

a natural frequency of the order of 300 c.p.s.

and deflections of 10^{-4} inches at full load

output of the 1 h.p. test motor.

The final calculated values of natural frequency and deflection (appendix 1) are:

natural frequency = 289 cycles per second

deflection at full load = $8.5 \cdot 10^{-5}$ inches.

When measured subsequent to construction, the values of these quantities were found to be:

natural frequency = 345 cycles per second

deflection at full load of the order of $7 \cdot 10^{-5}$ inches.

The difference of approximately 16% between the measured and calculated values for the natural frequency could be due to the use of incorrect values for Young's Modulus for the metals concerned, together with possible variations and inaccuracies in the dimensions of the portions of the apparatus involved in the calculations.

2.2. Description of Suspension System.

The suspended motor is shown in fig. 2. The rotor is supported independently of the stator to minimize the inertia of the deflecting system. The stator windings and laminations have been removed from the motor housing and are supported by four steel straps welded to a clamping ring and rigidly attached to a cast iron yoke.

The stator movement is due to the reaction of the rotor on the stator and is restricted to a purely rotational movement.

4. CHARACTERISTICS OF THE TEST MOTOR DURING THE STARTING PERIOD. IN THE ABSENCE OF SWITCHING TRANSIENTS.

4.1. Experimental Procedure to Eliminate Switching Transients.

The test motor was driven at full speed in the reverse direction by means of the 5 h.p. D.C. motor and the 50 c.p.s. A.C. supply circuit was completed. After allowing the supply to attain its steady state values, the D.C. motor was disengaged allowing the test motor to accelerate.

The oscillograms of fig. 5 represent torque, current and speed against time for the accelerating period.

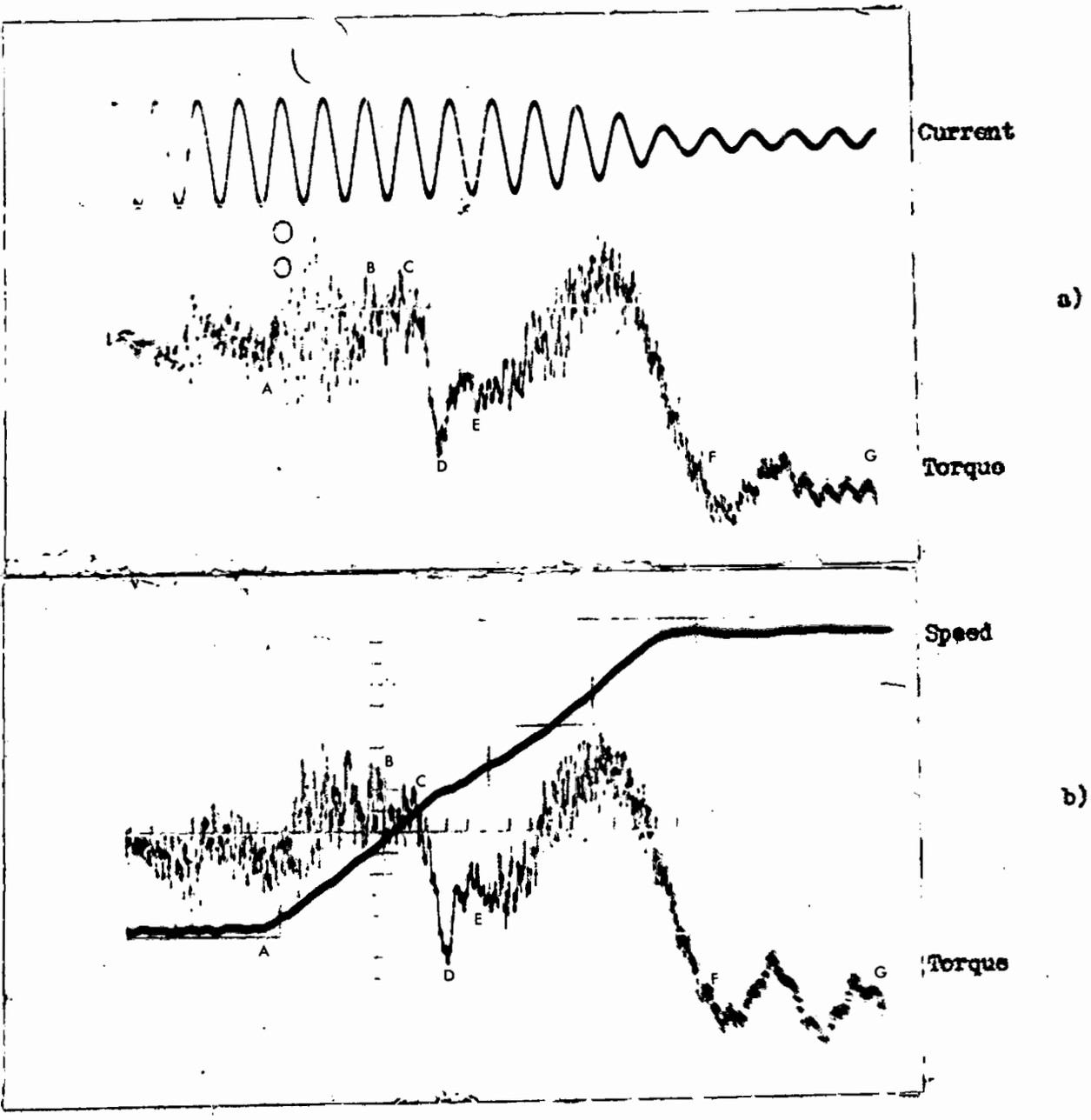

Fig. 5. Torque, speed and current versus time for plugged start of test motor with squirrel cage rotor.

Thus the deflection of the stator is proportional to the torque output of the motor and is independent of the type of load.

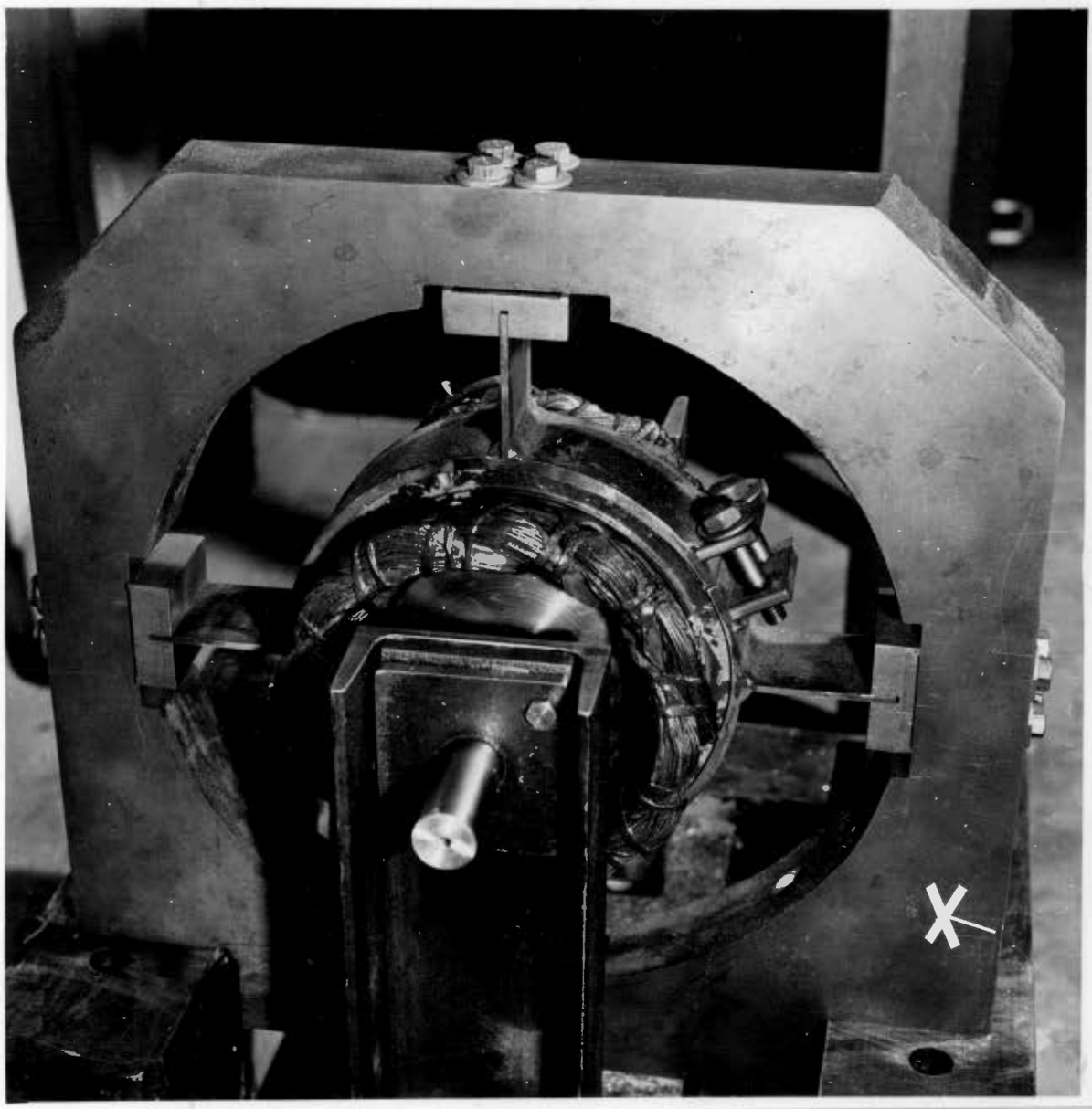

Fig. 2. Test motor with solid rotor suspended in cast iron yoke. Position for deflection measuring unit at point 'X'.

2.3. Control Apparatus.

A Ward-Leonard controlled 5 h.p. D.C. motor is used to maintain a constant speed, or to control the rate of acceleration, when required. When not required, a dog clutch is disengaged, mechanically isolating the test motor.

The instant at which the 380 volt 3-phase supply is connected to the stator of the test motor, may be controlled over

180 degrees relative to the supply voltage. The control is effected by means of a thyratron-operated contactor. The firing pulse to the thyratron is supplied from a phase-shifting device (appendix 2).

The accuracy of the switching control is dependent upon the consistency of operation of the contactor, and has been found to be suitable by recording several operations of the apparatus at the same setting.

2.4. Effect and Treatment of Suspension System Natural Frequency.

The initial test results obtained showed that the response of the equipment was suitable in general, but that the clarity of the oscillograms of torque was adversely affected by the amplitude of the vibrations at the natural frequency of the system. It had been expected that this frequency of vibration would be excited by the slot frequency vibrations but the effect of these vibrations had been underestimated. The frequency of the vibrations due to the slots is dependent upon the rotor speed and can be shown to be:[8]

$$f_s = \frac{Sr \cdot N}{60} \qquad \text{----------(2)}$$

where

f_s = frequency of stator vibrations

Sr = number of rotor slots

N = r.p.m.

To reduce the effect of the amplification factor (Q) of the mechanical system, of the order of 80, a frequency trap has been incorporated in the torque recording circuit. The frequency trap consists of a series tuned circuit shunting the oscilloscope input terminals.

The combined frequency response curve (appendix 3) shows that the overall response of the system is 3 dB up at 345 c.p.s. and suitably level elsewhere.

2.5. Measurement of Deflection and Speed.

The stator rotational deflection is used to deflect the diaphragm of a tuned cavity in a microwave system (appendix 4). The relationship between the deflection of the diaphragm and the output from the cavity is linear over the working range. Variations in the cavity output power due to deflections estimated to be less than 10^{-5} inches have been recorded. The system is calibrated by applying a known torque to the stator and recording the deflection of the oscillograph trace.

A homopolar generator designed and built for the investigation (appendix 5), is directly coupled to the shaft of the test motor. The output from the generator is of the order of 1 millivolt per rev. per second and is ripple-free.

The output from each of these measuring devices is fed into a D.C. low drift differential amplifier with a gain of the order of 100. A slight drift of the torque trace can be observed after a period of several minutes, but over the longest testing time, of the order of 500 milli-seconds, this drift is negligible.

2.6. Behaviour of Apparatus.

Fig. 3 is presented as an example of the recording properties of the equipment. The analysis of results follows at a later stage. The oscillogram of fig. 3a represents torque and speed against time for direct-on starting of the test motor. For a pure inertia load, acceleration is proportional to torque, as in this case if bearing friction and windage can be neglected. Thus the corroboration between the measured and derived curves of speed of fig. 3b illustrates the suitability of operation of the equipment. The derived values of fig. 3b were obtained by graphically integrating the torque trace of fig. 3a.

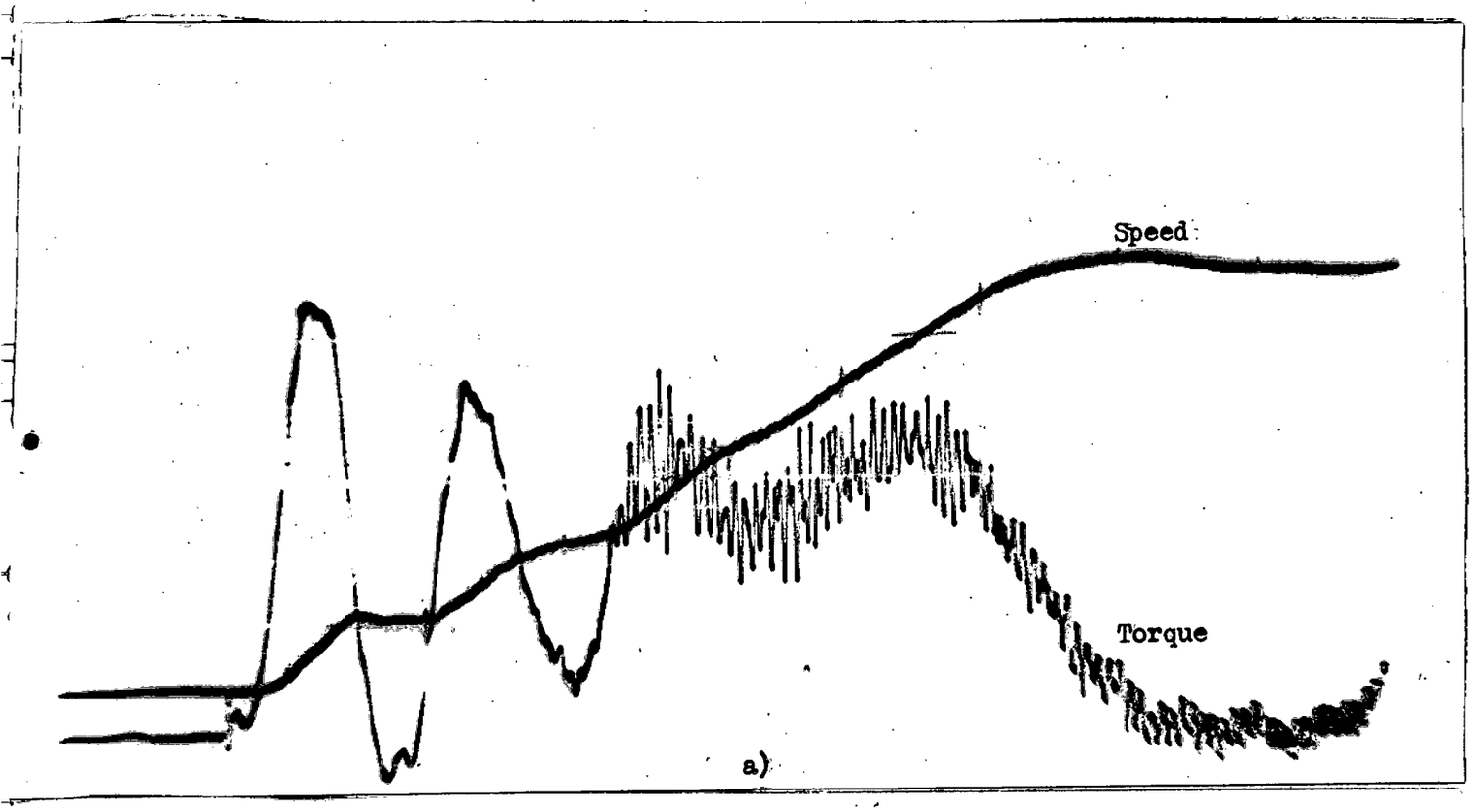

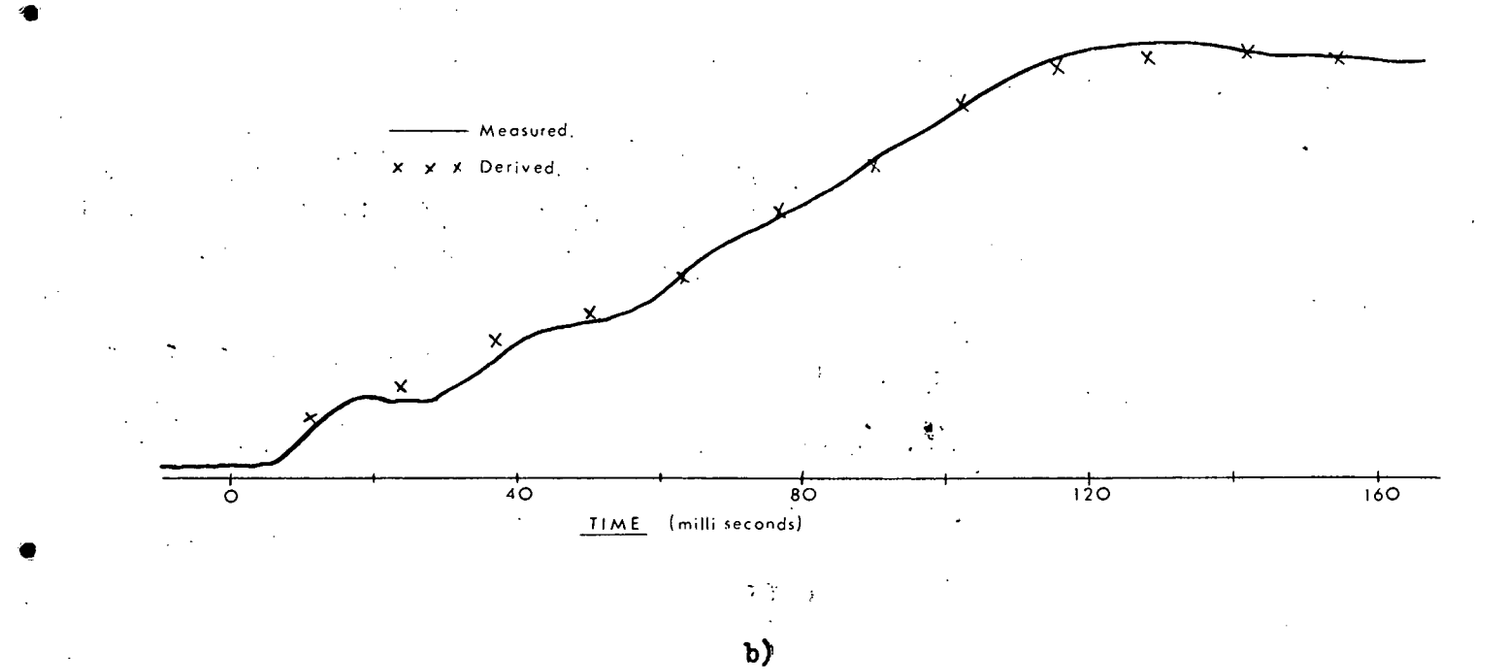

Fig. 3. Direct-on starting of test motor with squirrel cage rotor.

3. THE COMPLETE TORQUE AND SPEED CHARACTERISTICS OF THE TEST MOTOR WITH A SQUIRREL CAGE ROTOR.

With the apparatus as described, oscillograms of torque and speed against time over the range slip = 2 to slip = 0 were taken with a squirrel cage rotor. The complete oscillogram is shown in fig. 4a. To simplify the interpretation of the oscillogram, fig. 4b and fig. 4c show a separation of the expected characteristics from those obtained experimentally. The components of the curve are tabulated in table 2 and dealt with individually.

TABLE 2. OBSERVATIONS MADE FROM FIG. 4.

	FIGURE	SECTION	OBSERVATIONS
i)	4a	E-F	Low frequency torque pulsations
ii)	4a	F	Transient overspeeding
iii)	4a	E-F	High frequency vibration superimposed on the torque trace
iv)	4c	E & F	Harmonic torques
v)	4a & 4b	C-D	Deviation of recorded torque from expected theoretical torque-time characteristic
vi)	4a & 4b	A-B	Torque pulsations due to influence of transient switching currents.[6,13]

For convenience, the analysis of the observations given in table 2 will be undertaken in two distinct stages. The first stage will deal with the torque, current and speed variations with time during the starting period, excluding the influence of transient switching currents. The second stage will deal with the torque and current variations with time, under the influence of transient switching currents at different constant speeds.

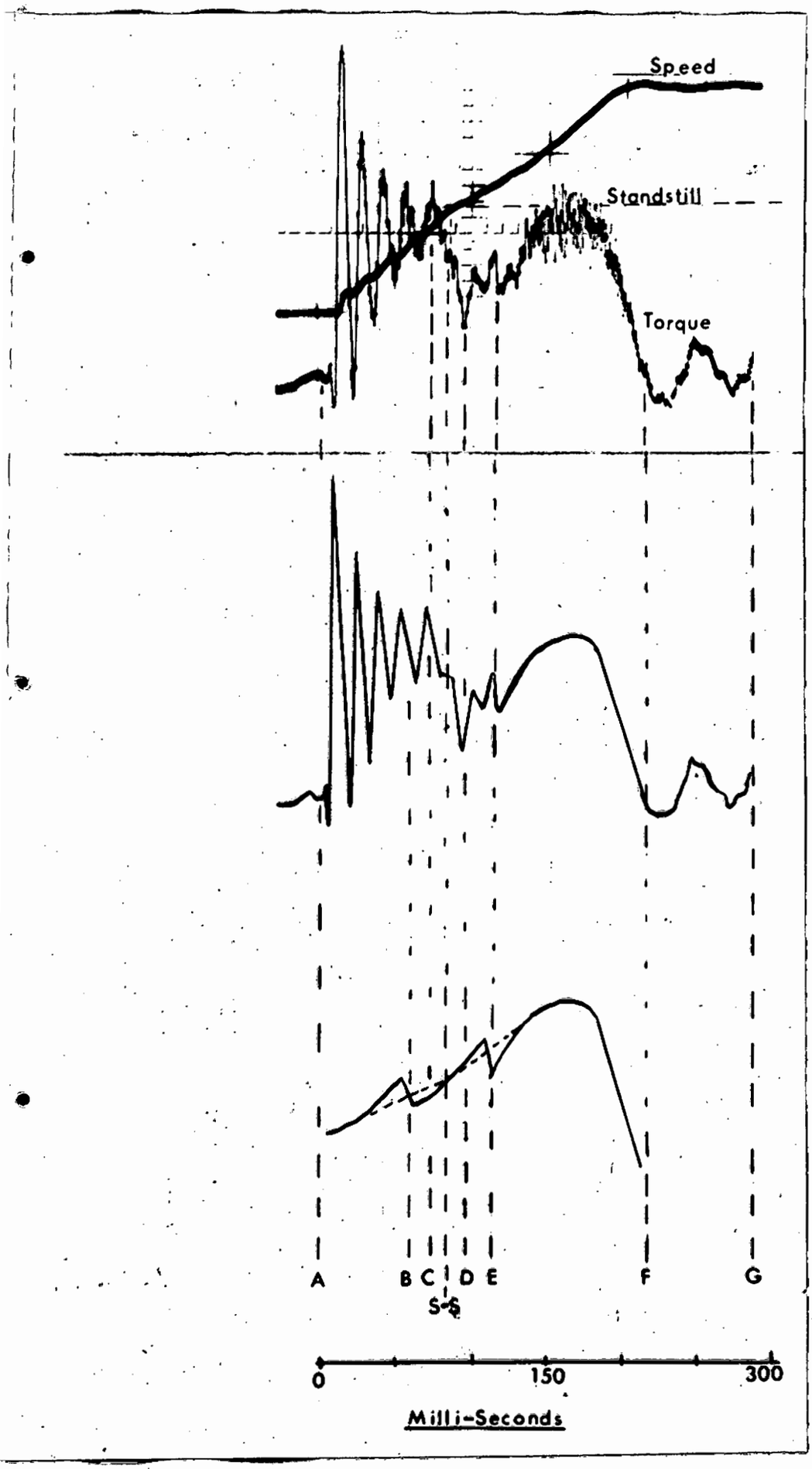

a) Actual oscillogram

b) Torque omitting higher frequencies

c) Expected steady state torque showing 5^{th} and 7^{th} harmonics

Fig. 4. Complete plugged start of test motor.

4.2. Discussion of Results.

The sequence of table 2 will be used for the purpose of this discussion.

4.2.1. Low frequency torque pulsations.

The torque traces of fig. 5, in the region corresponding to F-G of fig. 4, clearly show 25 c.p.s. pulsations with superimposed 100 c.p.s. vibrations. The 25 c.p.s. torque pulsation is due to rotor eccentricity for a 4 pole motor and varies continuously in magnitude at the rotor slip frequency. Comparison of the torque traces of fig. 5 shows the extent of the variations in magnitude. The superimposed 100 c.p.s. vibrations are a result of the deflections of the stator, produced magnetically by the 50 c.p.s. supply.

4.2.2. Transient overspeeding.

The transient overspeeding of induction motors has frequently been observed during the testing of lightly loaded machines[10, 11, 12] and can be used as an argument that transient conditions persist throughout the accelerating period, long after any initial switching transients have decayed.

It can be shown[10] that the transient overspeeding is due to the frequency modulation of the air gap flux over the period subsequent to the instant corresponding to maximum torque (T_{max}). Over the same period, the current trace of fig. 5a provides an example of frequency modulation as the motor current phase angle changes rapidly from approximately 45° at T_{max} to an angle of the order of 70° at no load.

4.2.3. High frequency vibration superimposed on the torque trace.

The relative motion of the stator and rotor slots produces vibrations in the stator[8] of a frequency as given by equation 2 section 2.4.

$$f_s = \frac{Sr\ N}{60}$$

Where Sr = rotor slots = 33

N = r.p.m.

Hence at a speed of 1200 r.p.m. the frequency of vibration would be 660 c.p.s.

In addition to the above, vibrations are produced by the harmonics of the fundamental stator flux and harmonics of the fundamental rotor flux in the air gap.[9]

The magnitude of the resultant vibrations, as shown in the oscillograms of fig. 5, is an indication of the noise produced by the motor during starting.

4.2.4. Harmonic torques.

The variations in torque, due to the 7^{th} harmonic torque in the forward direction and the 5^{th} harmonic torque in the reverse direction,[13] are shown in the oscillograms of fig. 5 in the positions corresponding to B and E of fig. 4 at speeds corresponding to $-N_s/5$ and $N_s/7$.

4.2.5. The deviation of the recorded torque over the stand-still region from the expected theoretical torque-time characteristic.

With reference to the sudden decrease in torque over the stand-still region[7, 11] as shown by the torque traces of fig. 5, in the region corresponding to C-D of fig. 4, the following information has been obtained experimentally.

i) This decrease in torque is independent of any switching transient effects by reason of the conditions under which the results were obtained.

ii) This torque decrease is produced irrespective of the rate and direction of acceleration of the rotor, as shown by the oscillograms of fig. 6. The results shown in fig. 6 are portions of an oscillogram for which the rotor was driven both with and against its own direction of acceleration by means of the Ward-Leonard controlled D.C. motor. The time taken to traverse the speed range from full speed in one direction to full speed in the other, is of the order of 2 seconds as compared with an acceleration time of the order of 250 milli-seconds in the case of free acceleration.

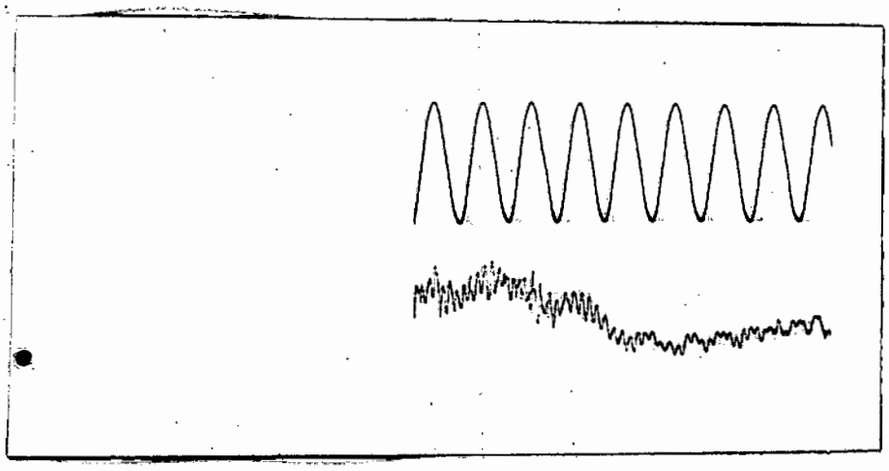

Current 50 c.p.s.

a) Forward

Torque

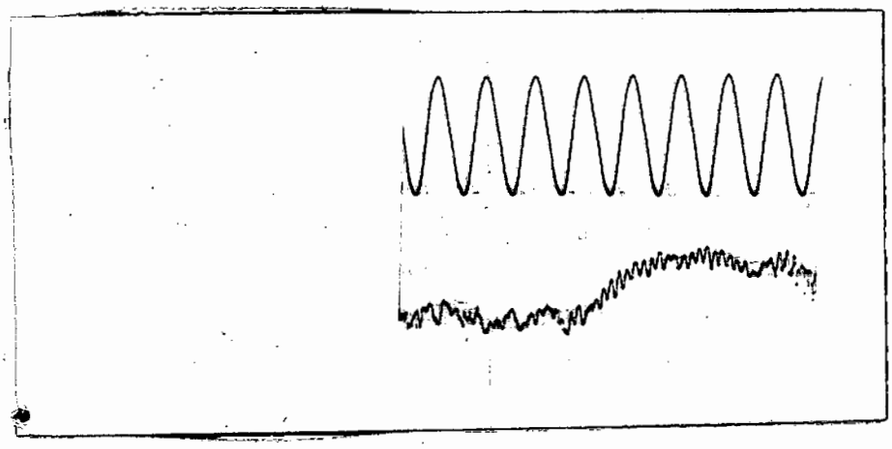

Current 50 c.p.s.

b) Reverse

Torque

Fig. 6. Controlled acceleration over stand-still region.

iii) Finally, the squirrel cage rotor was replaced by a solid rotor and the oscillogram shown in fig. 7 obtained under the same conditions as for fig. 5.

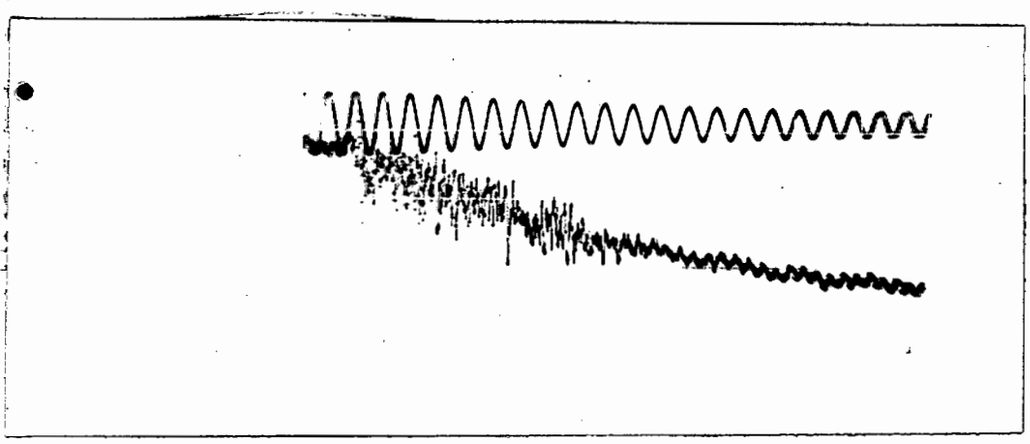

Current 50 c.p.s.

Torque

Fig. 7. Plugged start, excluding switching transients, for test motor with solid rotor.

The torque time relationship of the test motor with a solid rotor is that of an induction motor with a high resistance rotor, and no longer shows variations in torque over the region C-D or the influence of slotting.

An explanation which has been given for the variations in torque over the region C-D for a squirrel cage motor is that it is due to harmonic induction torques.[13] The test motor with 4 poles and 24 stator slots will produce primarily the 11^{th} and 13^{th} harmonics of the fundamental stator flux in the air gap, and their effect on the torque would be observed at -1/11 and 1/13 of synchronous speed.

The effects of these harmonics is reduced by the fact that there are 33 rotor bars and that the rotor bars are skewed. If there was no skewing and 44 rotor bars, the effect of the 11^{th} harmonic would be a maximum, and for 52 rotor bars the effect of the 13^{th} harmonic would be a maximum, as in each of these cases adjacent rotor bars would be under opposite poles of the harmonic flux.[13] The effect of either harmonic would be a minimum if the angle of skewing of the rotor bars was such that each bar spanned one pole pitch of the harmonic wave. Here the angle of skew of the rotor bars is 10^{o} and so each bar will have a span of 0.61 poles of the 11^{th} harmonic flux wave and 0.72 poles of the 13^{th} harmonic flux wave.[14]

Fig. 8 illustrates the effect of the 11^{th} and 13^{th} harmonics in a 4 pole squirrel cage induction motor with 24 stator slots and, 26 rotor slots in fig. 8a, and 44 rotor slots in fig. 8b, and unspecified angle of skew.[13]

Comparison of figs. 8a and 8b shows the augmenting effect of the rotor slotting on the harmonic torques. However, these torques would be expected to be associated with relatively small variations in slip, unlike the results shown in fig. 5 where the torque trace has been influenced over the region slip = 2 to slip = 1.

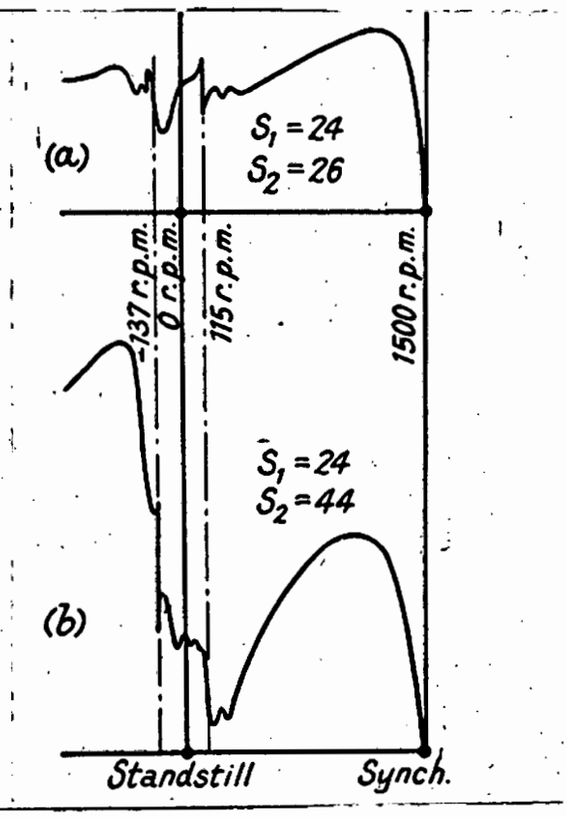

Fig. 8. Torque/speed curves of 4 pole 50-cycle motor.[13]

Further investigation is being made with respect to this variation in torque in an attempt to determine its cause or causes conclusively. One portion of the investigation involves the modification of the squirrel cage rotor to provide facilities for observing the individual rotor bar currents, and another involves the substitution of a wound rotor for the cage rotor, as a wound rotor tends to reduce the effects of most harmonics of pole-pitch different from the coil pitch, while an unskewed cage rotor will circulate the current related to any harmonic except that which has a pole-pitch equal to the pitch of the rotor bars.

5. THE INFLUENCE OF TRANSIENT SWITCHING CURRENTS ON THE TORQUE OF THE TEST MOTOR.

The term 'transient switching currents' has been used on several occasions previously and refers to the exponentially decaying currents initiated at the instant of completion of a circuit containing resistance and inductance. The expression for the instantaneous current in a single phase resistive and inductive circuit is:[15]

$$i = I_{max} \sin(\omega t - \alpha) - I_{max} e^{\frac{R}{L}(t'-t)} \sin(\omega t' - \alpha) \quad ----(3)$$

where the time, t', is measured from the instant at which the voltage wave is zero, and at the instant of completion of the circuit $t = t'$ secs.

The first term on the right-hand side of the equation represents the steady state current and the second term on the right-hand side of the equation represents the transient switching currents.

At the instant of completing the three-phase A.C. supply circuit to the stator of an induction motor, the boundary conditions are that the current in each phase, and the magnetic flux in the machine, must be zero.[3]

It can be shown[3, 16] that these conditions necessitate a transient m.m.f. excited by decaying direct currents in the stator winding, in addition to the normal revolving m.m.f. produced by the steady state currents. The transient m.m.f. is stationary in space since it is produced by unidirectional currents flowing through stationary coils, and is equal and opposite to the revolving m.m.f. at the instant of switching. The resultant flux at this instant is therefore zero.

When the entire three-phase system of currents in the stator windings is considered, it is not necessary to consider the phasing of the instant of switching relative to the supply,[17] as any variation in the instant of switching relative to the supply

only varies the space location of the transient m.m.f. and does not vary its initial magnitude.

This was confirmed by taking several oscillograms at different instants of switching.

The simultaneous existence of a stationary transient m.m.f. and a steady state revolving m.m.f. in the stator, as mentioned above, has been simulated by the test described in the following section.

5.1. Torque Produced under the Combined Influence of Steady State Direct and Alternating Current Supplies.

The speed of the energized test motor was kept constant at preselected values by means of the 5 h.p. Ward-Leonard controlled D.C. motor, and a direct current was injected at the stator star-point, as shown in fig. 9, without upsetting the symmetry of the A.C. supply. Table 3 summarizes the observations made from the oscillograms of fig. 10 taken during the steady state under the above conditions.

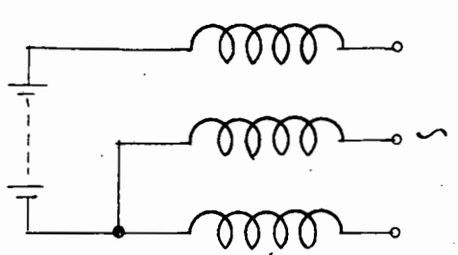

Fig. 9. Circuit diagram for test described in section 5.1.

TABLE 3. SUMMARY OF RESULTS FLOW FIG. 10.

SLIP	2	1 (APPROXIMATE SPEED = 23 R.P.M.)	0
FREQUENCY OF TORQUE PULSATIONS (C.P.S.)	50 + 25	50 + 12.5	50 + 25
CURRENT PULSATIONS	Nil	Nil	Nil

a) Slip = 2

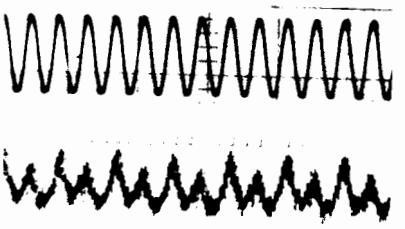

Current 50 c.p.s.

Torque

b) Slip = 1
(speed = 23 r.p.m.)

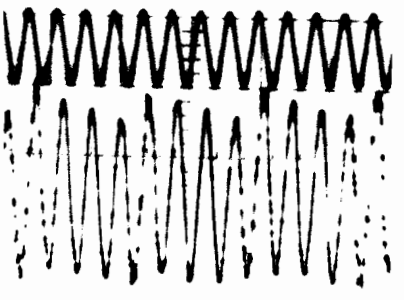

Current 50 c.p.s.
(applied direct current halved)

Torque

c) Slip = 0

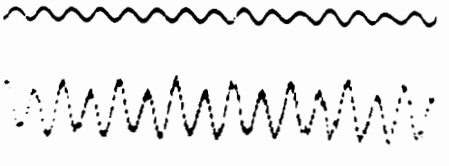

Current 50 c.p.s.

Torque

Fig. 10. Torque and current for combined steady state alternating and direct currents.

5.1.1. Analysis of oscillograms of fig. 10.

The simultaneous existence in the stator of the revolving alternating current excited m.m.f. with the stationary direct current excited m.m.f. results in a pulsating torque. The amplitude of the pulsations are dependent upon the rotor speed relative to the stator fields, as the armature reaction effect of the rotor increases with the relative speed. This is illustrated by the smaller amplitudes of the torque pulsations in fig. 10a and 10c.

The main frequency of pulsation is shown to be 50 c.p.s. irrespective of rotor speed. The superimposed 12½ c.p.s. pulsation shown in fig. 10b is a result of variation of the leakage inductance due to slotting, and is produced by a measured rotation of the order of 23 r.p.m. (for 33 rotor slots:- $\frac{12.5 \times 60}{33} = 22.7$ r.p.m.) In the case of the oscillograms of fig. 10a and 10c, the superimposed 25 c.p.s. pulsation is due to the eccentricity of the rotor as discussed in section 4.2.1.

To analyse the production of torque under the above conditions, consider first the individual actions of these m.m.f.s and their corresponding fluxes, noting that torque is proportional to[19]

(The linking flux)x(rotor current)x(cosine of the angle between flux and current)

Therefore, when a mutual flux ϕ and a current I rotate synchronously with one another, the torque produced is unidirectional and is proportional to

$$\phi \, I \cos \theta$$

However, when the flux and current rotate asynchronously, a pulsating torque is produced. The frequency of pulsation is equal to the frequency of the relative rotation. For example, the torque produced by a flux ϕ' rotating with an angular velocity of ω, and a stationary current I", will be proportional to

$$\phi' \, I'' \cos \omega t$$

Fig. 11 shows the two sets of fluxes and stator and rotor currents separated into synchronous groups. Fig 11a represents the spatial relationships of the A.C. quantities and fig. 11b the D.C. quantities.

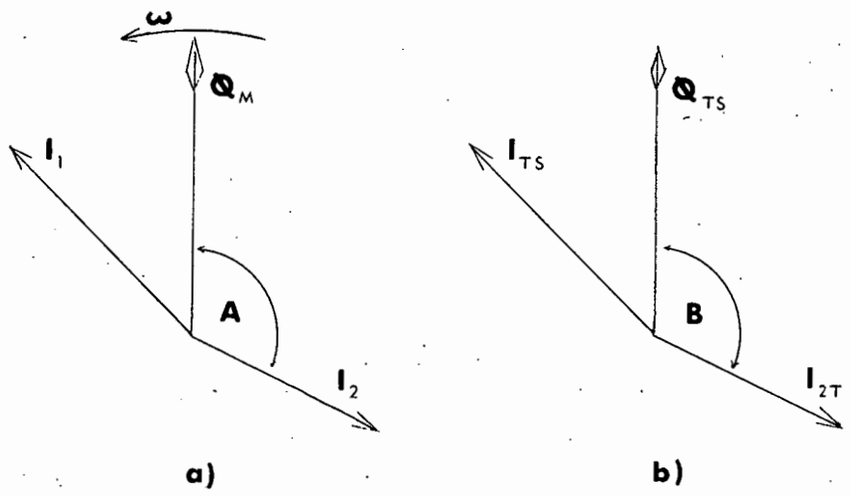

Fig. 11. Spatial relationships of fluxes and currents.

The synchronous and asynchronous components of torque produced by the components of fig. 11 will be as shown in table 4, where allowance is made for the initial spatial angle between the quantities involved in the asynchronous torques.

TABLE 4. COMPONENTS OF TORQUE PRODUCED BY THE STEADY STATE SUPERPOSITION OF D.C. UPON THE NORMAL A.C. SUPPLY.

	SYNCHRONOUS TORQUES	DIRECTION
i)	$\phi_m I_2 \cos A$	Forward
ii)	$\phi_{TS} I_{2T} \cos B$	Braking
	ASYNCHRONOUS TORQUES	PULSATION FREQUENCY
iii)	$\phi_m I_{2T} \cos(F \pm \omega t)$	Supply frequency
iv)	$\phi_{TS} I_2 \cos(G \pm \omega t)$	Supply frequency

where F and G are the initial phase angles between each pair of the fluxes and currents, and ω is the angular velocity of the A.C. revolving field.

The frequency of pulsation of the asynchronous torques as shown by table 4 is independent of the rotor speed and is equal to the frequency of the A.C. supply.

However, these results do not agree with the results obtained under actual switching conditions, as shown in the following section.

5.2. Torque Produced under Transient Switching Conditions.

The 1 h.p. test motor was connected to the 380 volt 50 c.p.s. 3-phase supply with the rotor speed kept constant at preselected values by means of the 5 h.p. Ward-Leonard controlled D.C. motor. The oscillograms of fig. 12 covering the duration of the switching transient currents, were recorded for each speed.

The relationships between the current and torque pulsations and the rotor speed, or slip, are summarized in table 5.

TABLE 5. SUMMARY OF RESULTS FROM FIG. 12.

SLIP	2	1.5	1	0.5	0
FREQUENCY OF TORQUE PULSATION (C.P.S.)	100	75	50	25	Exponential
APPROXIMATE DURATION OF PULSATIONS IN CYCLES AT 50 C.P.S.	$2\frac{1}{2}$	4	9	7	$2\frac{1}{2}$
MEAN TORQUE	Positive	Positive	Positive	Positive	Negative
FREQUENCY OF PULSATIONS ON MEAN (C.P.S.)	—	25	—	25	Exponential

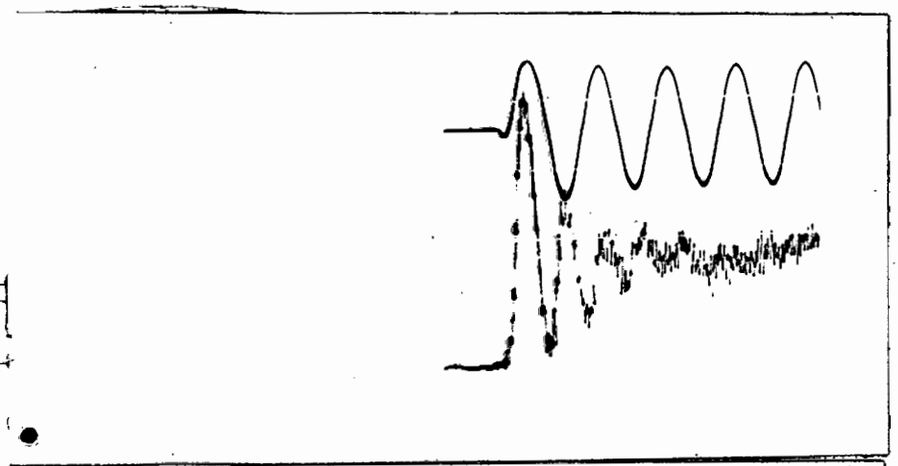

a) Slip = 2

Current 50 c.p.s.

Torque pulsations

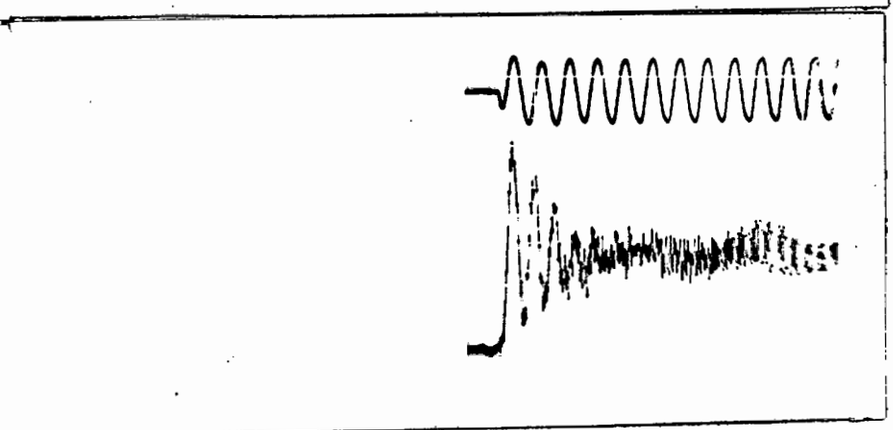

b) Slip = 1.5

Current 50 c.p.s.

Torque pulsations

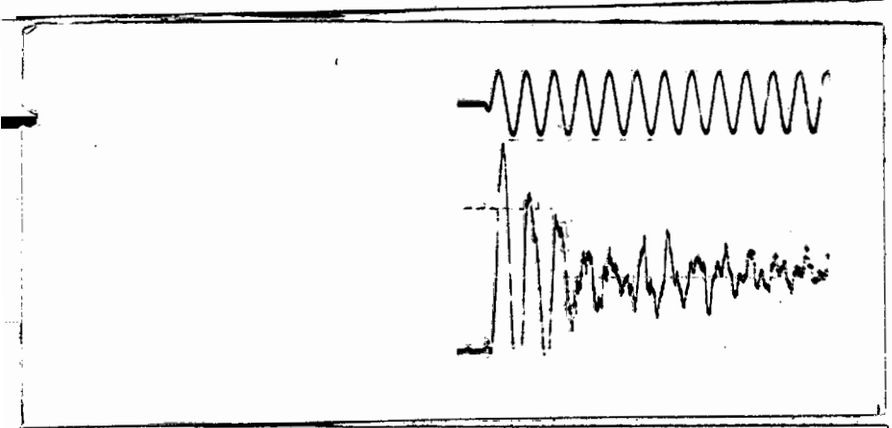

c) Slip = 1.0

Current 50 c.p.s.

Torque pulsations

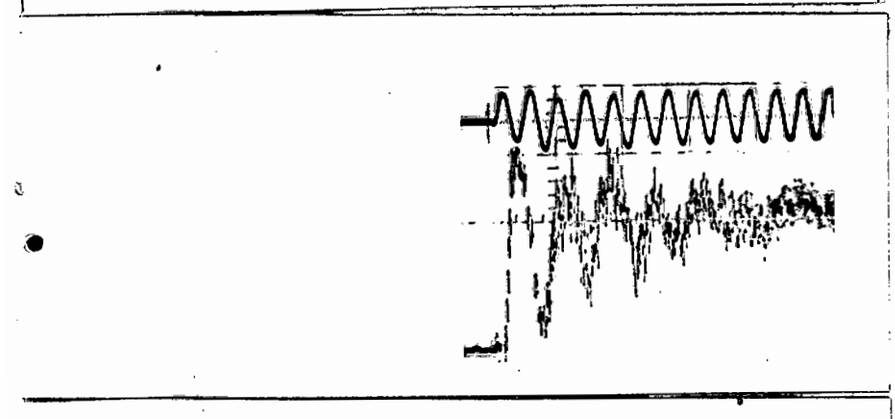

d) Slip = 0.5

Current 50 c.p.s.

Torque pulsations

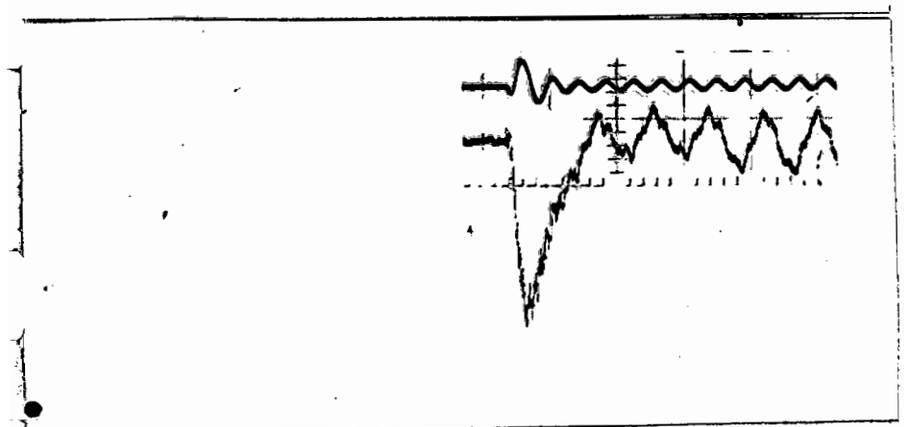

e) Slip = 0

Current 50 c.p.s.

Torque pulsations

Fig. 12. Torque and current under switching conditions.

5.2.1. Analysis of oscillograms of fig. 12.

The oscillograms of fig. 12 show that for the duration of the transient switching currents, produced when the stator is connected to the 3-phase 50 c.p.s. supply, the expected unidirectional torques have superimposed pulsations of a frequency given by:

$$f = (50 - \frac{PN}{60}) \text{ c.p.s.} \qquad \text{----------(4)}$$

where

P = pairs of poles

N = r.p.m. and is positive in the forward direction only.

These pulsations decay exponentially at a different rate for each case of constant speed, as shown in table 5.

Similarly, the current traces show superimposed pulsations at a frequency given by:

$$f = \frac{PN}{60} \text{ c.p.s.} \qquad \text{----------(5)}$$

where

N = r.p.m. and is positive for either direction of rotation.

It has been shown experimentally in section 5.1., and can be shown mathematically[6] that the combination in the stator of only a stationary field and a revolving field cannot result in the production of torque pulsations at any frequency other than that of the A.C. supply.

A condition which could provide the change in frequency of the torque pulsations related to the rotor speed as shown by equation 4, is one which would be produced by the simultaneous existence of the stator revolving m.m.f. and a m.m.f. carried by the rotor. Furthermore, the armature reaction effect of the stator windings with the flux produced by the rotor m.m.f., would superimpose pulsations on the stator current at a frequency given by equation 5.

Rudenberg,[18] shows that, based upon the solution to the equations pertaining to polyphase machines under switching conditions, there exist, in addition to the steady state stator revolving m.m.f. and its current systems in the stator and rotor,

two transient m.m.f.s and their current systems in the stator and rotor. One of the transient m.m.f.s adheres to the stator and the mutual flux it produces cuts the rotor windings at the speed of revolution of the rotor, while the other transient m.m.f. adheres to the rotor and the mutual flux it produces cuts the stator windings at the rotor speed.

The rates of decay of the transient m.m.f.s are controlled mainly by the leakage time constant (ratio of leakage inductance to resistance) of the stator or rotor winding to which the m.m.f. is adhering.

If the rotor time constant is larger than the stator time constant, the effect of the transient rotor adherent m.m.f. may still be evident after the stator switching transient quantities have decayed completely.[18]

To illustrate the production and effect of a rotor adherent m.m.f. the test described in the following section was carried out.

5.3. An Example of a Rotor Adherent M.M.F.

The speed of the test motor was maintained constant at previously selected values and impulses of direct current only were applied to the stator, as shown in fig.13.

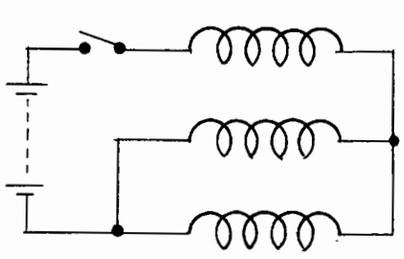

Fig. 13. Circuit diagram for test.

Table 6 summarizes the behaviour of the stator current at each speed, as shown by the oscillograms of fig. 14.

TABLE 6. SUMMARY OF RESULTS FROM FIG. 14.

SLIP	2	1.5	1	0.5	0
TOTAL RISE TIME IN CYCLES AT 50 C.P.S.	$2\frac{1}{2}$	8	$10\frac{1}{3}$	8	$2\frac{1}{2}$
INITIAL RISE (CYCLES RELATIVE TO 50 C.P.S.)	$\frac{1}{3}$	$\frac{1}{3}$	$\frac{1}{3}$	$\frac{1}{3}$	$\frac{1}{3}$
APPROXIMATE FREQUENCY OF PULSATION (C.P.S.)	50	25	Exponential rise only	25	50
DURATION OF PULSATION RELATIVE TO 50 C.P.S.	2	$7\frac{1}{2}$	10	$7\frac{1}{2}$	2

Referring to fig. 14 and table 6, it is evident that the current rise in each case shows a combination of two time constants. The initial rise time is the same in every case. It is shorter than the final rise time in each case and is associated with the stator leakage time constant.[18]

It is evident from the oscillograms of fig. 14 that the final rise of current is associated not only with the rotor leakage time constant but also with the rotor speed.[18] The relationship between the rotor time constant and the rotor speed is shown in appendix 6.

Fig. 14 also shows that during the final rise of stator current, the rotor acts in a similar fashion to the field-carrying system of an alternator, as illustrated by the pulsations superimposed on the stator current. These pulsations are synchronous with the rotor, and the frequency of pulsation is given by equation 5. It will be observed that the magnitude of these current pulsations decreases with increased rotor speed. This is consistent with a more rapid decay of the transient rotor adherent m.m.f. with increased rotor speed.

Taking into account the transient rotor adherent m.m.f., the production of the torques as shown by fig. 12 in section 5.2. is analysed.

5.4. Analysis of the Torques Produced in the Test Motor During the Influence of the Transient Switching Currents.

It has been shown that three m.m.f.s exist in the motor during the period of influence of the transient switching currents. These are the stator steady state revolving m.m.f., the transient stator adherent m.m.f. and the transient rotor adherent m.m.f.

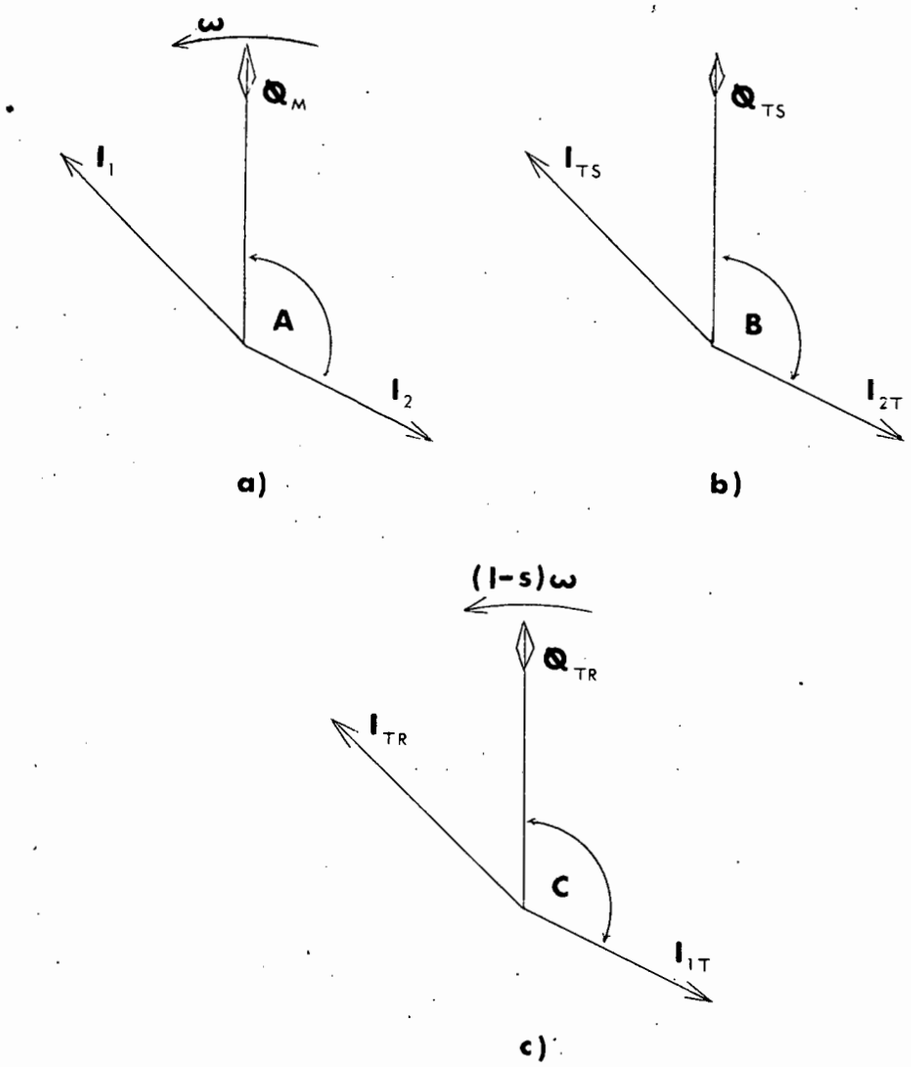

Fig. 15. Spatial relationships of fluxes and currents.

Fig. 15 shows the three sets of fluxes and currents separated into synchronous groups. Fig. 15a represents the spatial relationships of the supply frequency quantities. That is, the steady state relationship between the stator current I_1, mutual flux ϕ_m and resultant rotor current I_2.

The stationary quantities are shown in fig. 15b. These are the stator adherent transient current I_{TS}, the stationary transient stator adherent mutual flux ϕ_{TS} and the resultant rotor current I_{2T}.

The quantities revolving synchronously with the rotor are shown in fig. 15c. These are the transient rotor adherent current I_{TR}, the transient rotor adherent mutual flux ϕ_{TR} and the resulting stator current I_{1T}.

If the rate of decay of the stator transient quantities is represented by the term e^{-at}, and that of the rotor transient quantities by e^{-bt}, the synchronous and asynchronous components of torque produced by the components of fig. 15 will be as shown in table 7, where allowance is made for the initial spatial angle between the quantities involved in the asynchronous torques.

For the case of the test motor with a squirrel cage rotor, the relative magnitudes of the terms e^{-at} and e^{-bt} may be obtained from the results of table 6 and fig. 14. The term e^{-at} relates to the initial rate of rise of the current as shown by the oscillograms of fig. 14, and in all cases its duration is much shorter than that of the term e^{-bt} which relates to the final rate of rise. For this case therefore, the terms in table 7 involving e^{-at} may be neglected. This leaves only terms i), iii), iv) and v).

Term iii) is a braking torque and terms iv) and v) are asynchronous torques with a frequency of pulsation equal to the frequency of slip of the rotor relative to ϕ_m.

The frequencies of pulsation of the asynchronous torques are clearly in agreement with the frequencies of pulsation shown in fig. 12 with the possible exception of the case where the slip is zero.

TABLE 7. COMPONENTS OF TORQUE DURING THE PERIOD OF INFLUENCE OF TRANSIENT SWITCHING CURRENTS.

	SYNCHRONOUS TORQUES	DIRECTION OF TORQUE
i)	$\phi_m I_2 \cos A$	forward
ii)	$e^{-at} \phi_{TS} e^{-at} I_{2T} \cos B$	braking
iii)	$e^{-bt} \phi_{TR} e^{-bt} I_{1T} \cos C$	braking
	ASYNCHRONOUS TORQUES	FREQUENCY OF PULSATION
iv)	$\phi_m e^{-bt} I_{TR} \cos(D+S\omega t)$	frequency of slip of
v)	$e^{-bt} \phi_{TR} I_1 \cos(E+S\omega t)$	rotor relative to ϕ_m
vi)	$\phi_m e^{-at} I_{2T} \cos(F+\omega t)$	supply frequency
vii)	$e^{-at} \phi_{TS} I_2 \cos(G+\omega t)$	
viii)	$e^{-at} \phi_{TS} e^{-bt} I_{TR} \cos(H+(1-S)\omega t)$	frequency of rotation
ix)	$e^{-bt} \phi_{TR} e^{-at} I_{TS} \cos(K+(1-S)\omega t)$	of rotor

where

ϕ_m = steady state stator revolving flux

ϕ_{TS} = stationary stator adherent transient flux

ϕ_{TR} = transient rotor adherent flux

I_1 = stator steady state current

I_{TS} = stator adherent transient current

I_{1T} = stator current due to ϕ_{TR}

I_2 = rotor current due to ϕ_m

I_{TR} = transient rotor adherent current

I_{2T} = rotor current due to ϕ_{TS}

a = stator effective damping exponent (Appendix 6)

b = rotor effective damping exponent (Appendix 6)

D, E, F, G, H and K are the initial spatial phase angles between each pair of quantities producing asynchronous torques.

When the slip is zero, only the terms iii), iv), and v) of table 7 need be considered, as the steady state torque must be zero. By inspection, the resultant of terms iii), iv) and v) must be an exponentially decaying torque. However, consideration of the boundary conditions shows that the torque must start from zero, and inspection of the actual transient torque produced at zero slip, as shown by fig. 12e which is presented again, enlarged, as fig. 16, shows that the torque increases to a negative maximum before decaying.

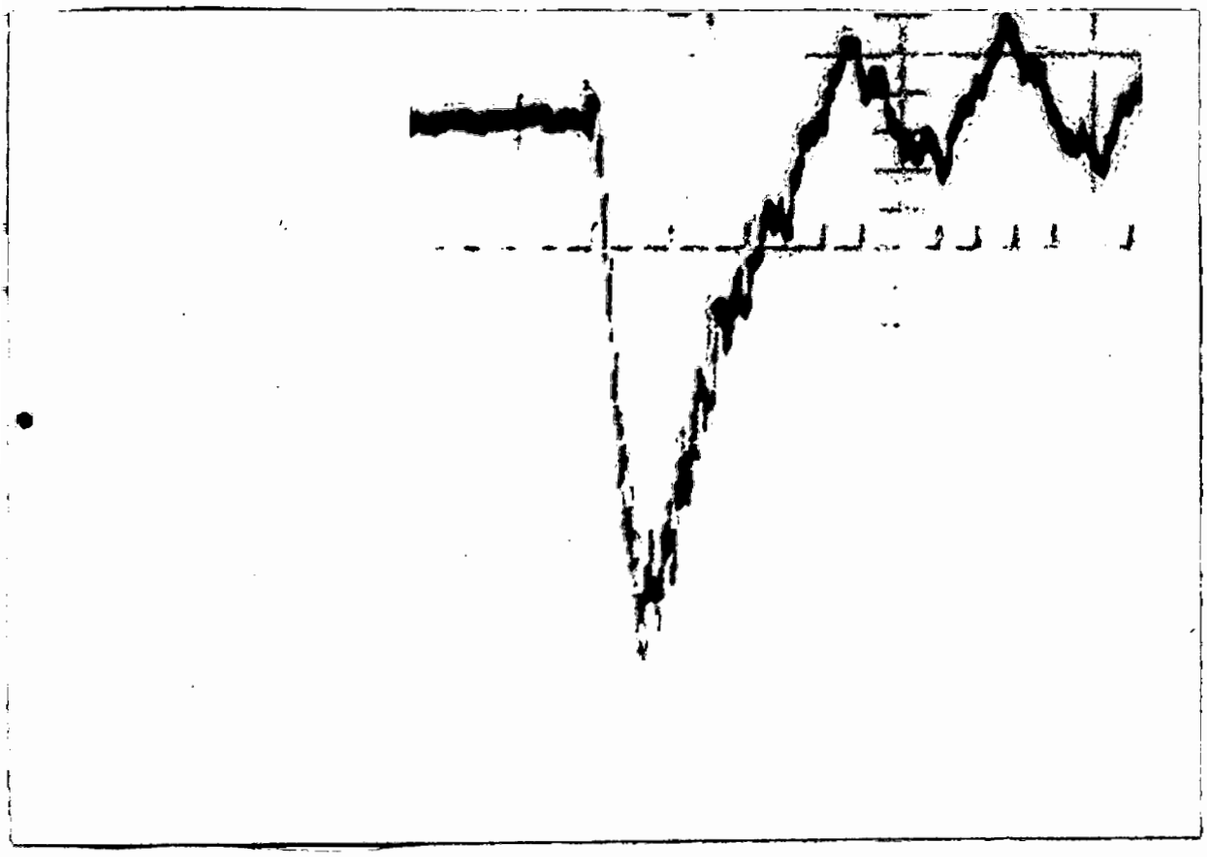

Fig. 16. Transient switching torque vs time at zero slip.
(Time scale 50 milli-seconds per inch)

To find the law of the curve of torque, the curve of Log Torque vs Time was drawn, as shown by fig. 17. This shows that over the period A-B of fig. 17 the negative torque decays exponentially, agreeing with the resultant of the components of table 7.

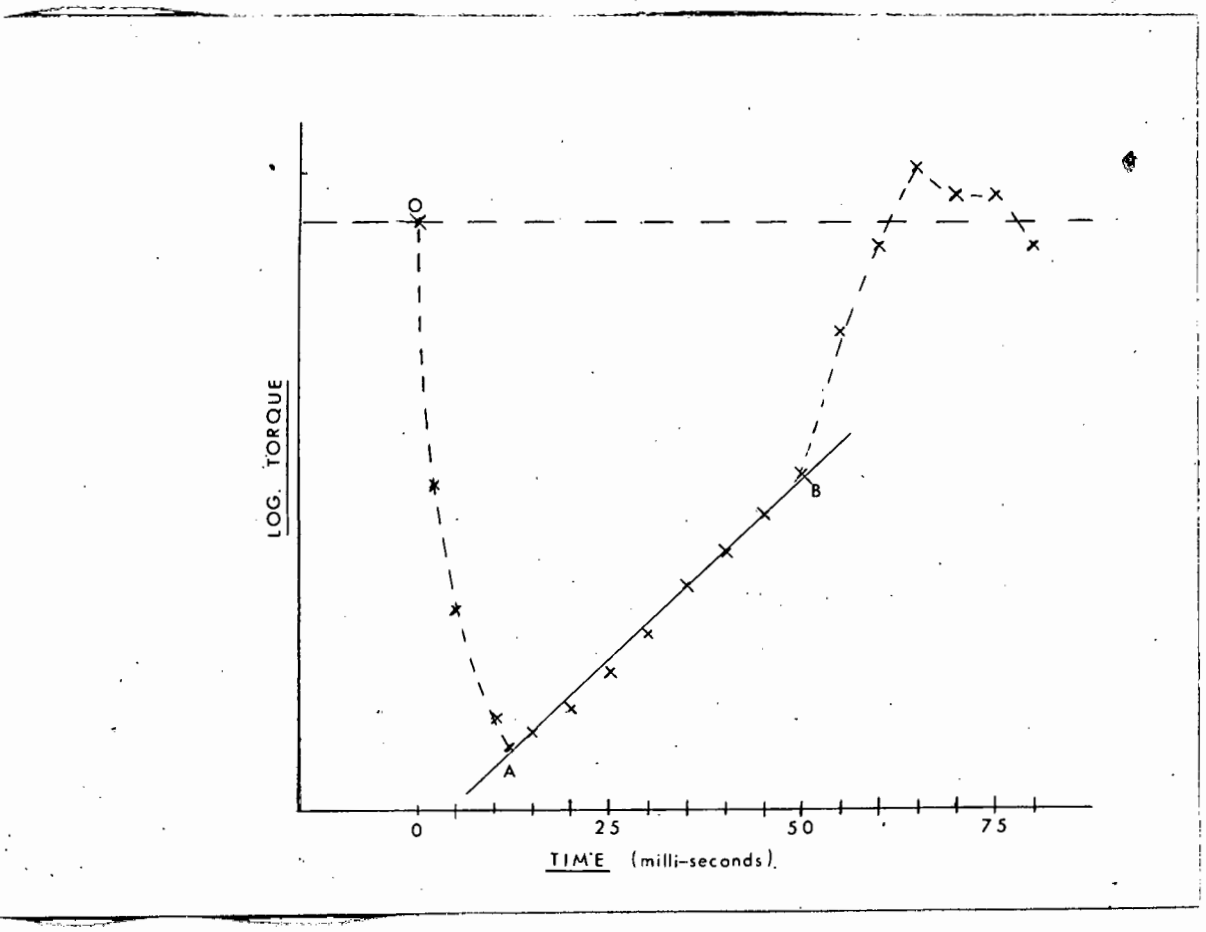

Fig. 17. Log. transient switching torque vs time at zero slip.

However, consideration of only terms iii), iv) and v) of table 7 will not produce the increase in negative torque as shown in the period O-A of fig. 17. This indicates that the terms of table 7 involving the decay rate of e^{-at} should be considered if the transient torque produced during the first 10 milli-seconds of operation is to be investigated. The torque produced after the point B (approximately 55 milli-seconds after switching) is mainly the steady state torque variation due to the rotor eccentricity as mentioned in section 4.2.1.

These results indicate that the resultant of the components of torque of table 7 describes the torque produced during the switching period, provided that the stator transient quantities decay rapidly with respect to the rotor transient quantities, and only after the decay of the stator transient quantities. It should be noted that a rapid decay of the stator transients would explain the apparent absence of supply frequency

pulsations on the oscillograms of torque of fig. 12.

In the case where the rotor transient quantities decay rapidly with respect to the stator transients the above description of the resultant torque will no longer hold. To illustrate this case, tests were made as described in the following section.

5.5. Transient Switching Torques Produced by the Test Motor with a Solid Steel Rotor.

A solid steel rotor was substituted for the squirrel cage rotor and the test motor was connected to the 380 volt 50 c.p.s. 3-phase supply at several constant speeds, as described in section 5.1.1. The oscillograms of fig. 18 cover the duration of the transient switching currents for each speed, and the observations made from these results are given in table 8.

The fact that motors with solid rotors have peculiar characteristics due to the variations in the permeability and the resistivity of the rotor during starting[21] is not taken into account here, as the predominant effect is that of a high resistance rotor.

TABLE 8. SUMMARY OF RESULTS FROM FIG. 18.

SLIP	2	1.5	1	0.5	0
APPROXIMATE FREQUENCY OF TORQUE PULSATION (C.P.S.)					
a) First ½ cycle	100	75	50	25	Exponential
b) Subsequent to first ½ cycle	50	50	50	50	50
APPROXIMATE DURATION OF PULSATIONS IN CYCLES AT 50 C.P.S.	3	4	5+		3

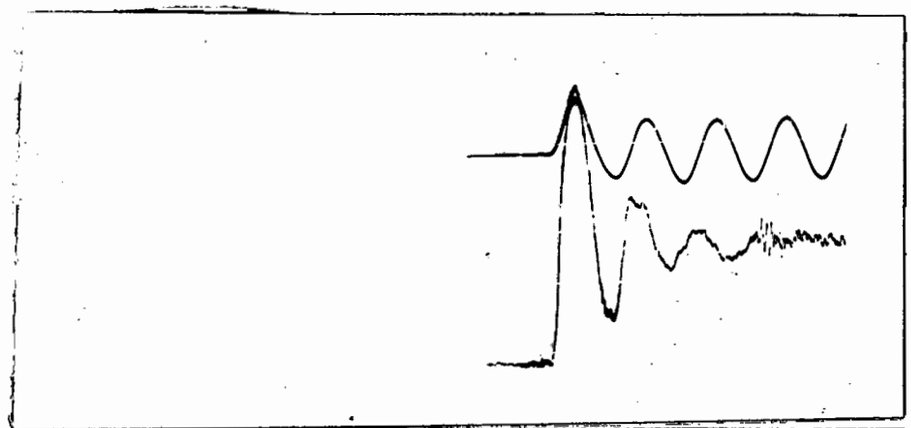

a) Slip = 2

Current 50 c.p.s.

Torque pulsations

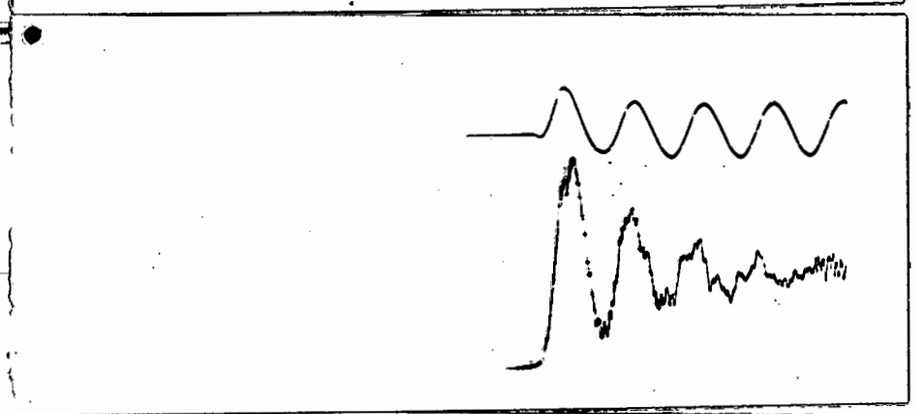

b) Slip = 1.5

Current 50 c.p.s.

Torque pulsations

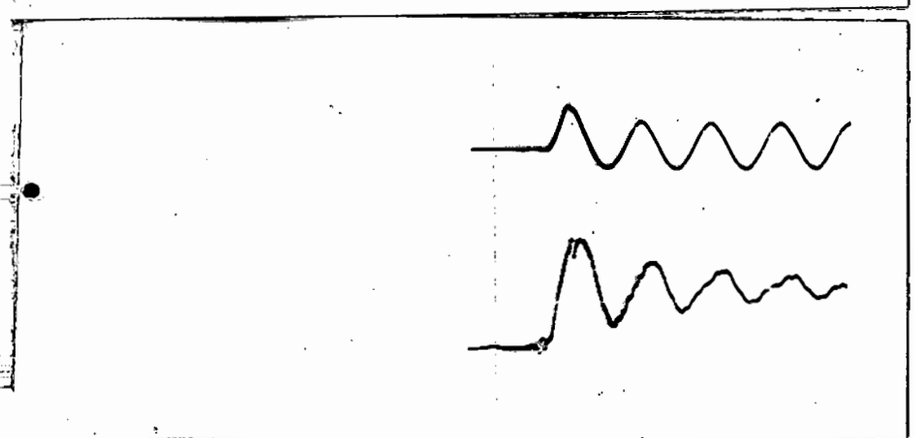

c) Slip = 1

Current 50 c.p.s.

Torque pulsations

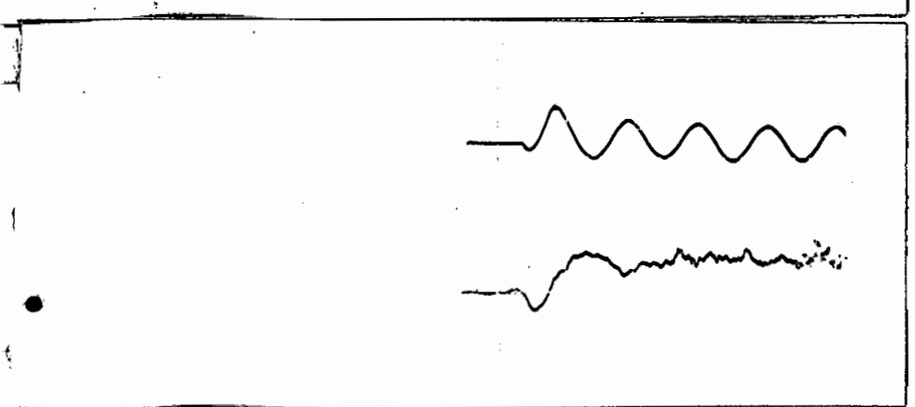

d) Slip = 0.5

Current 50 c.p.s.

Torque pulsations

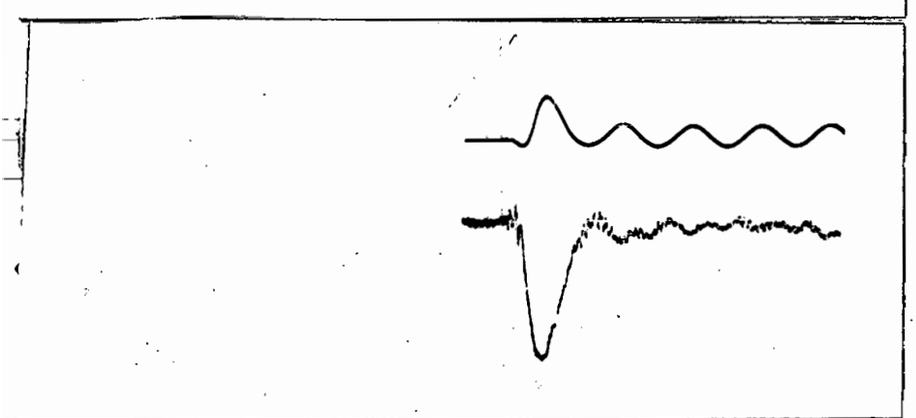

e) Slip = 0

Current 50 c.p.s.

Torque pulsations

Fig. 18. Torque and current of solid rotor motor under switching conditions.

Inspection of table 7 shows that if all the terms involving the rate of decay e^{-bt} are neglected, the frequency of the pulsating torques superimposed upon the unidirectional torques is the same as the supply frequency. This corresponds to the results of fig. 18 subsequent to the first ½ cycle after the instant of switching.

A rapid decay of the rotor transient quantities in comparison to the rate of decay of the stator transient quantities is consistent with a rotor of sufficiently high resistance.

Briefly, the above results together with those of section 5.3. show that when the transient rotor adherent m.m.f. is of long duration in comparison to the stationary transient stator adherent m.m.f., the resultant pulsations superimposed upon the unidirectional torque are of slip frequency. However, when the duration of the transient rotor adherent m.m.f. is short compared with the transient stator adherent m.m.f., the resultant pulsations are at the supply frequency.

6. CONCLUSIONS.

i) The torque measuring apparatus used provides a means of investigating the more rapid variations in torque, such as those produced by an induction motor under transient switching conditions.

ii) The results obtained from the investigation of the torque/speed characteristic of the squirrel cage induction motor, excluding the influence of transient switching currents, verify the results obtained by previous investigators. In particular, the deviation of the measured characteristic, from slip = 2 to slip = 1, from the theoretical characteristic deserves further investigation.

iii) Under switching conditions there exist, in addition to the steady state stator revolving m.m.f. and the related systems of currents in the stator and rotor, a stationary transient m.m.f. which adheres to the stator, and a further transient m.m.f. which adheres to the rotor. The rates of decay of the transient stator and rotor adherent m.m.f.s are controlled primarily by the leakage time constant of the stator and rotor respectively.

This verifies the theoretical analysis produced by Rudenberg.[18]

iv) During the period of influence of the transient currents initiated at the instant of switching, pulsations are superimposed upon the unidirectional steady state torques. The magnitude of these torque pulsations may be twice the pull-out torque or more.

v) Where the rotor leakage time constant is short relative to the stator leakage time constant, the frequency of the transient switching torque pulsations is equal to the supply frequency subsequent to the decay of the rotor adherent transient quantities. Under these conditions, results approximating to the values as calculated by Gilfillan and Kaplan[2] could be obtained.

vi) Where the rotor leakage time constant is long relative to that of the stator, the experimental results obtained show a

departure from the results of previous investigators in that the predominant frequency of pulsation of the transient switching torques is that of the frequency of the slip of the rotor relative to the steady state stator revolving field.

vii) The results obtained substantiate the experimental results of Wahl and Kilgore[6] for the case where the slip = 1. For this case the frequency of pulsation of the transient switching torques is equal to that of the supply, irrespective of the ratio of the stator and rotor leakage time constants.

7. ACKNOWLEDGMENTS.

My acknowledgements and sincere thanks are due to the following:

Dr. N.C. de V. Enslin who supervised this thesis and who gave advice and suggestions, detailed criticism and invaluable assistance at all stages of the experimental work and in the final preparation of the manuscript;

Professor R.W. Guelke, Professor of Electrical Engineering, for his constant encouragement and advice throughout this thesis;

Messrs. J.N. Wright and D. Kenyon of the Department of Electrical Engineering workshops, for their willing assistance in the construction of the apparatus.

8. BIBLIOGRAPHY.

1) STANLEY H.C. — An Analysis of the Induction Machine. Transactions A.I.E.E. 1938, Vol. 57, p. 751.

2) GILFILLAN E.S. & KAPLAN E.L. — Transient Torques in Squirrel Cage Induction Motors, with Special Reference to Plugging. Transactions A.I.E.E. 1941, Vol. 60, p. 1201.

3) SMITH G.S. — Transients in A.C. Motors and Generators. Transactions A.I.E.E. 1946, Vol. 65, p. 61.

4) WEYGANDT C.N. & CHARP S. — Electromechanical Transient Performance of Induction Motors. Transactions A.I.E.E. 1946, Vol. 65, p. 1000.

5) MAGINNIS F.G. & SCHULTZ N.R. — Transient Performance of Induction Motors. Transactions A.I.E.E. 1944, Vol. 63, p. 641.

6) WAHL A.H. & KILGORE L.A. — Transient Starting Torques in Induction Motors. Transactions A.I.E.E. 1940, Vol. 59, p. 603.

7) CORMACK W. — The Measurement of the Torque-Slip Curves of Induction Motors. Transactions S.A.I.E.E. May 1955, Vol. 46, Part 5, p. 129-131.

8) LAGRON L. — Polyphase Induction Motors. (Blackie and Son, 1931), p. 52.

9) MORRIL W.J. — Harmonic Theory of Noise in Induction Motors. Transactions A.I.E.E. 1940, Vol. 59, p. 474.

10) AGEN R.W. — Transient Overspeeding of Induction Motors. Transactions A.I.E.E. 1941, Vol. 60 p. 1030.

11) HILL V. — Discussion on Ref. 7.

12) RAWCLIFFE G.H. & ASHWORTH A.F.H. — Induction Motor Speed Changing by Pole-Amplitude Modulation. A.E.I. Engineering, June 1961, Vol. 1, No. 6, p. 220-227.

13) SAY M.G. — The Performance and Design of Alternating Current Machines. (Pitman, 1958), p. 305-307.

14) STILL A. & SISKIND C.S. — Elements of Electrical Machine Design. (McGraw-Hill, 1954), p. 281.

15) GOLDING E.W. — Electrical Measurements and Measuring Systems. (Pitman, 1957), p. 592.

16) RUDENBERG R. — Transient Performance of Electric Power Systems. (McGraw-Hill, 1950), p. 236.

17) RUDENBERG R. Transient Performance of Electric Power Systems. (McGraw-Hill, 1950), p. 147-148.

18) RUDENBERG R. Transient Performance of Electric Power Systems. (McGraw-Hill, 1950), p. 134-146.

19) COTTON H. Electrical Technology. (Pitman, 1957), p. 557.

20) SAY M.G. The Performance and Design of Alternating Current Machines. (Pitman, 1958), p. 621.

21) GIBBS W.J. Induction and Synchronous Motors with Unlaminated Rotors. Journal I.E.E. 1948, Vol. 95, Part II, No. 46, p. 411.

22) ROARK R.J. Formulas for Stress and Strain. (McGraw-Hill, 1938), p. 176 (Table X).

23) ENSLIN N.C. de V. A Method of Using Microwaves for Measuring Small Displacements, and a Torque-Meter Using this Principle. Proceedings I.E.E. 1954, Vol. 101, No. 83, Part II, p. 522-528.

24) JOHNSON C.C. A Homopolar Tachometer for Servo-Mechanism Application. Proceedings I.R.E. 1952, Vol. 40, p. 158.

Appendix 1. Stiffness and Natural Frequency of Supporting System.

i) Stiffness of supporting straps.

a) Loading due to displacement only of one support.

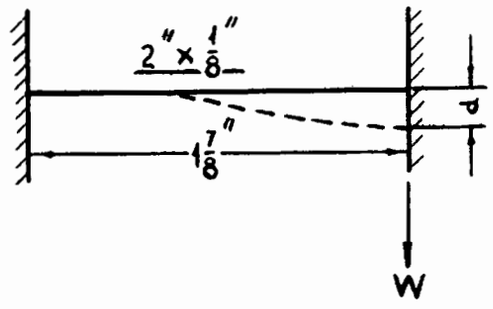

Assuming a deflection of 2×10^{-4} inches and having

$$d = \frac{W \ell^3}{12 EI}$$

where

$$I = \frac{2(1/8)^3}{12}$$

$E = 28 \times 10^6$ lbs/square inch

$W = 3.33$ lbs.

Bending moment

$$M_1 = \tfrac{1}{2} W \ell$$

$$= 0.5 \times 3.33 \times 1.875$$

$$= 3.12 \text{ lb-inches.}$$

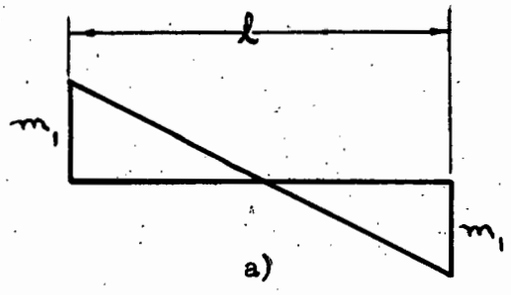

a)

b) Loading due to rotational movement of one end of support.

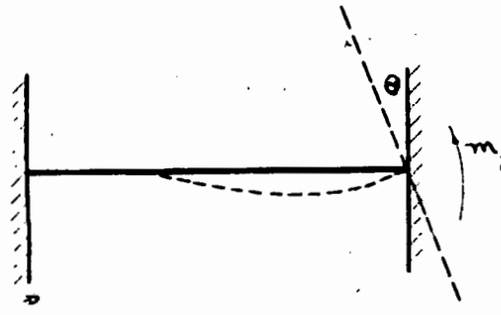

For a deflection of 2×10^{-4} inches at the circumference of the stator, radius = 3.75 inches

$$\theta = \frac{2 \times 10^{-4}}{3.75} \text{ radian}$$

$$M_2 = \frac{4EI\theta}{\ell} = 1.04 \text{ lb-inches}$$

and shear force

$$= \frac{(M_1 + \tfrac{1}{2}M_2) + (M_1 + M_2)}{\ell}$$

$$= \frac{3.64 + 4.16}{1.875}$$

$$= 4.16 \text{ lbs.}$$

Total torque required to deflect 4 supports 2×10^{-4} inches

$$= 4 \times 4.16 \times 3.75$$

$$= 62.4 \text{ lb-inches.}$$

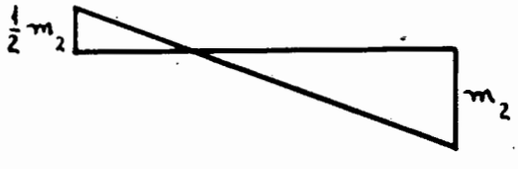

b)

Fig. 19. Loading of one support.

ii) Stiffness due to brass diaphragm.[22]

$$y_{max} = \frac{W \times 3(m^2 - 1)}{4\pi m^2 E t^3}\left[a^2 - b^2 - \frac{4a^2b^2}{a^2 - b^2}(\log_e a/b)^2\right]$$

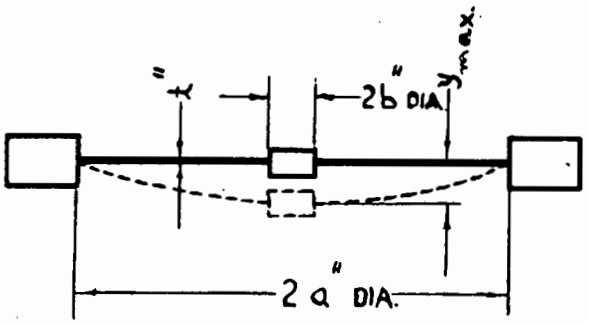

Fig. 20. Loading of diaphragm.

where

a = 1 inch

b = 0.3125 inches

t = 0.0625 inches

E = 13 x 10^6 lbs/square inch

$\frac{1}{m}$ = poissons's ratio

$m = \frac{1}{0.33} = 3$

and for a deflection of y_{max}

= 2 x 10^{-4} inches.

W = 8.47 lbs

Torque required to deflect diaphragm

= 8.47 x 4.25

= 36 lb-inches.

(neglecting any horizontal movement of the stator and any effect of the extension or bending of the rod).

Total torque required for a deflection of 2 x 10^{-4} inches of the stator equivalent to a rotation of θ radians,

T = 62.4 + 36

= 98.4 lb-inches.

Specific torque

$= T/\theta$

$= \frac{98.4 \times 3.75}{2 \times 10^{-4}}$

= 185 x 10^4 lb-inches/radian.

iii) Natural frequency of system.

$$f_o = \frac{1}{2\pi} \times \sqrt{\frac{T/\theta \times g}{I}}$$

(where $g = 32.14$ at U.C.T.)

The moment of inertia of the stator only, was determined experimentally by finding the period of oscillation when suspended by a bifilar system, and weighed to determine the mass. The moments of inertia of the relevant portions of the suspension system about the axis of rotation of the stator were calculated.

The total moment of inertia was estimated as 217 lb-inches.^{2}

$$f_o = \frac{1}{2\pi} \times \sqrt{\frac{185 \times 10^4 (32.14 \times 12)}{217}}$$

= 289 cycles per second.

The measured natural frequency of the system

= 345 cycles per second.

and the stiffness estimated from tests as

= 226 lb-inches/radian.

Using the value for the moment of inertia, as in the previous calculation, this value of stiffness agrees with the value required to produce a frequency of 345 cycles per second to within 5%.

The calculated natural frequency differs from the measured value by approximately 16%. This difference could be due to the use of incorrect values of the constants of the metals concerned, particularly with respect to the heating and quenching of the welded portions of the suspension system. Furthermore, the calculations are based upon the assumption of idealized deflections, and the extension of any portion of the suspension system during the rotational deflection of the stator has been neglected.

Appendix 2. Switching Instant Control.

Fig. 21 shows the circuit used to provide control of the switching instant. The zener diode produces a square wave which is differentiated forming positive and negative pulses. Once the switch S has been closed, the thyratron will only conduct after receiving a positive pulse from the phase shifting circuit, and on conducting, allows the contactor pull-in coil to be energised.

The contactor can also be operated normally by the local push buttons.

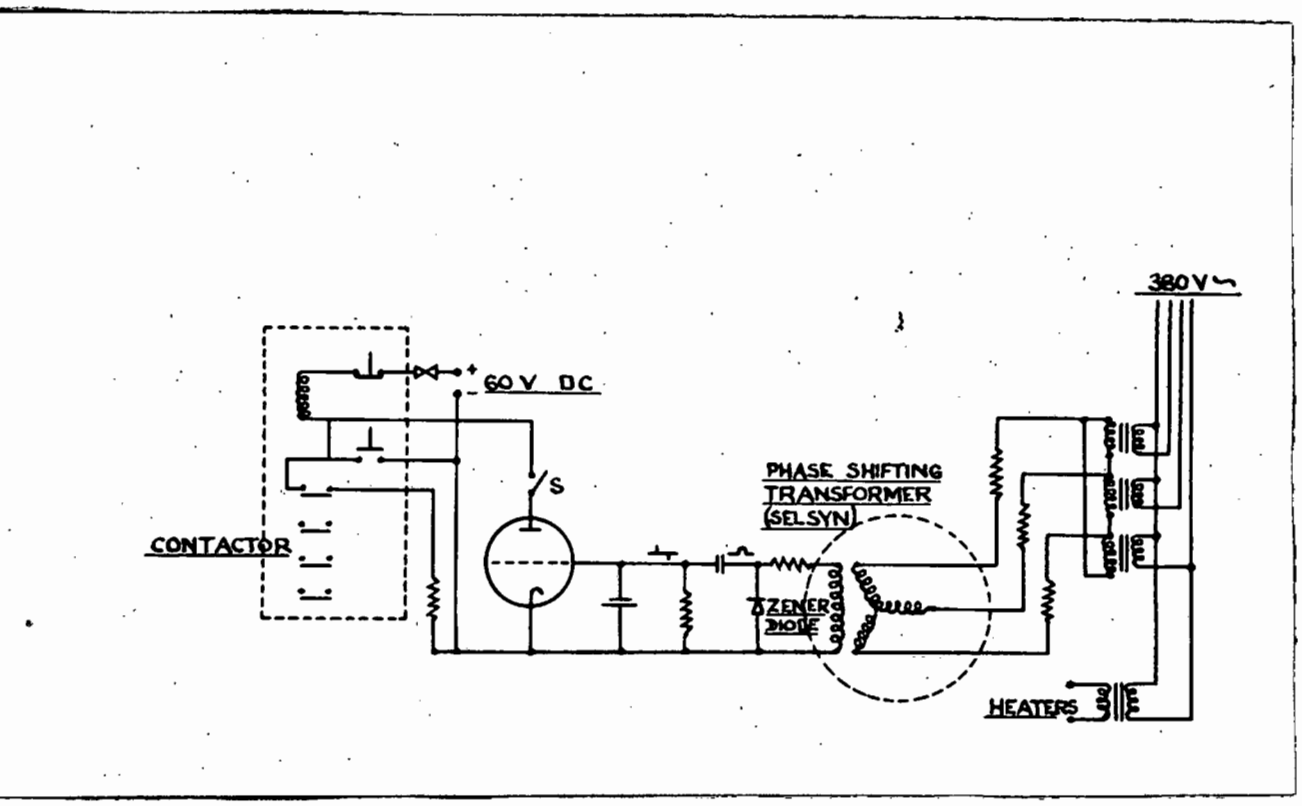

Fig. 21. Circuit diagram for switching instant control.

Appendix 3. Frequency Trap.

Fig. 22a gives the component values of the frequency trap and fig. 22b shows the relative response curves of the suspension structure, the frequency trap and their resultant relative response curve in the region of 345 c.p.s.

As the output impedence of the D.C. amplifier is very low, the Q of the frequency trap is also dependent upon the value of the series resistor. The maximum value of this resistor is limited by the fact that too high a resistance value in conjunction with the impedence of the frequency trap results in a noticeable drop in response at lower frequencies of interest.

With the resistance value as shown the frequency response is within 2.5% up to 150 c.p.s. rising to 3 dB up at 345 c.p.s.

The curve of the resultant response is obtained by dividing the amplitude of the structure relative response curve by that of the trap relative response curve.

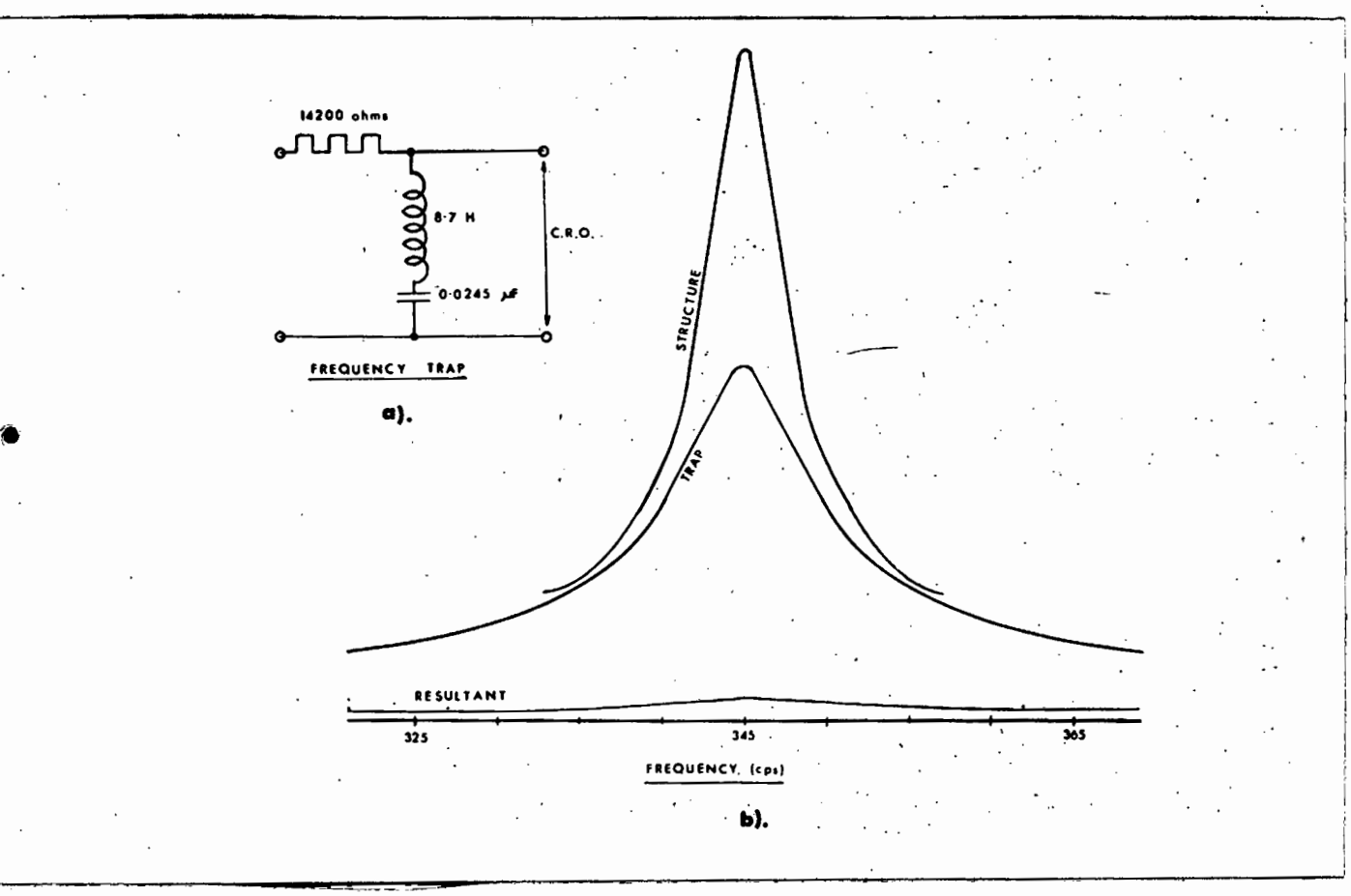

Fig. 22. Frequency trap and relative response curves.

Appendix 4. Measurement of Deflection.

The use of microwaves for measuring small displacements has been thoroughly dealt with[23] and here only a brief description of the operation of the resonant cavity is given.

Fig. 23a shows a cylindrical cavity closed at one end by an adjustable plunger so that the length of the cavity, x, can be altered. Input and output points are provided near the base of the cavity.

If power at a fixed frequency is fed into the cavity and the output connected to a crystal detector which measures the power transmitted through the cavity, then by varying the dimension x the curve shown in fig. 23b is obtained. If the cavity is set to point B corresponding to the plunger position x_b for an oscillator frequency which makes x_a the resonant point, there is a linear relationship between plunger displacement and transmitted power over the range $x_d - x_c$.

In the measuring system employed, the base of the cavity has been replaced by a diaphragm, shown in fig. 20, rigidly coupled to the stator of the test motor in such a way that any small rotational movement of the stator produces a proportional deflection of the diaphragm. Before each test the plunger is adjusted to point B ensuring a linear relation between displacement and cavity output.

Fig. 1 illustrates the layout of the microwave equipment.

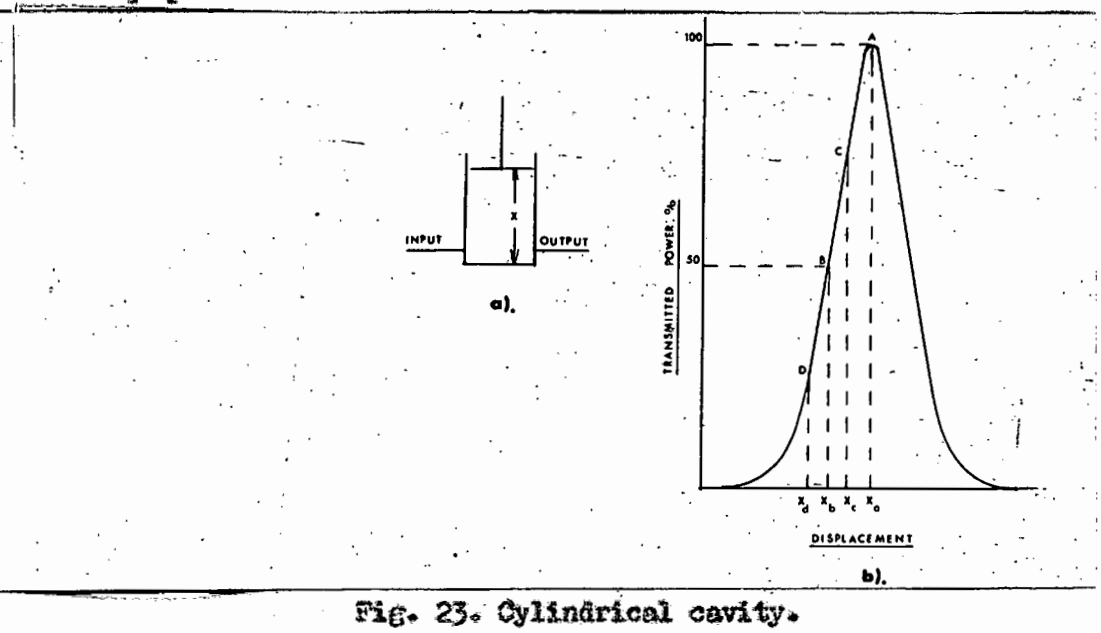

Fig. 23. Cylindrical cavity.

Appendix 5. Speed Measurement.

A homopolar generator is used to provide a ripple-free D.C. e.m.f. proportional to rotational speed. The e.m.f. output from this type of generator is unfortunately limited by the fact that the equivalent of one conductor only is rotated in a uniform magnetic field, and so for recording purposes the output is fed into a D.C. amplifier with a gain of the order of 100. The output from the generator is of the order of 1 millivolt per rev. per second with an excitation current of 0.36 amperes.

Fig. 24, while not to scale, shows a sectioned view of the generator. The air gap is 60×10^{-3} inches and the brass disc thickness is 30×10^{-3} inches. The coil consists of 1250 turns of 22 s.w.g. copper wire and the brushes are carbon.

It was expected that the use of carbon brushes on the brass disc would produce a thermal e.m.f., but it has been found that if any thermal e.m.f. is produced during the short running periods used in the tests, it is negligible in comparison with the rotational e.m.f. generated.

The generator mounting is fixed to the cylindrical body of the generator and the two end plates are accurately fitted and located on the body so that the removal of either or both end plates does not upset the lining up of the generator. The end plates are each secured by 6 x 6 B.A. screws, the front end plate carries the disc and circumferential brushes and the rear end plate the central pole piece and brush, and the exciting coil.

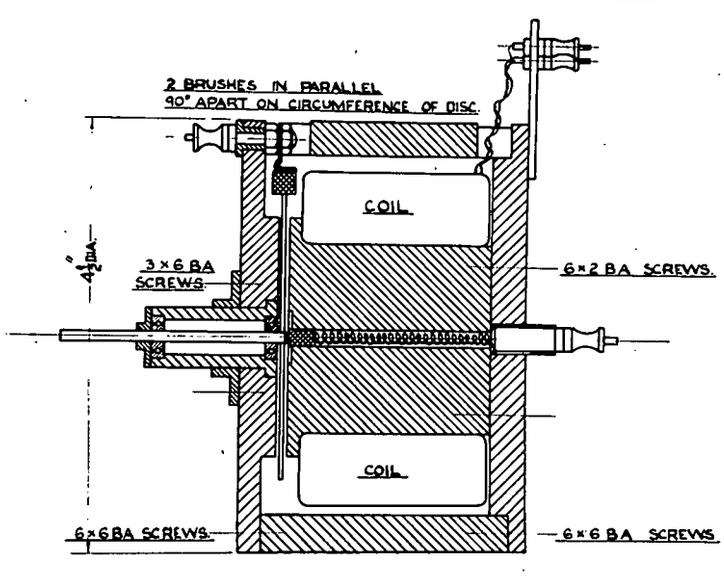

Fig. 24. Homopolar generator.

Appendix 6. Relationship between Rotor Speed and Stator and Rotor Time Constants.

Rudenberg[18] has shown that the relationship between rotor speed and stator and rotor time constants is as follows:

$$a = \frac{1}{T_1} = d' + \frac{d'' d'^2 (1 - D)}{\nu^2 + d'^2}$$

and

$$b = \frac{1}{T_2} = d'' - \frac{d'' d'^2 (1 - D)}{\nu^2 + d'^2}$$

where

a = stator effective damping exponent

b = rotor effective damping exponent

T_1 = resultant stator time constant

T_2 = resultant rotor time constant

ν = angular velocity of rotor

D = total leakage coefficient of the machine

$= 1 - \frac{M^2}{L_1 L_2}$

L_1 = stator inductance

L_2 = rotor inductance

M = mutual inductance

d' = stator damping exponent = $\frac{R_1}{D L_1}$

d'' = rotor damping exponent = $\frac{R_2}{D L_2}$

R_1 = stator resistance

R_2 = rotor resistance

For a squirrel cage induction motor d' is generally much larger than d'', in which case it follows from the above, that the stator time constant will be less affected by the rotor speed than the rotor time constant.